

NACA RM L54D20



# RESEARCH MEMORANDUM

INVESTIGATION AT HIGH SUBSONIC SPEEDS OF THE EFFECT OF  
ADDING VARIOUS COMBINATIONS OF MISSILES ON THE  
AERODYNAMIC CHARACTERISTICS OF SWEEPBACK  
AND UNSWEEP WINGS COMBINED  
WITH A FUSELAGE

By H. Norman Silvers and William J. Alford, Jr.

Langley Aeronautical Laboratory  
Langley Field, Va.

CLASSIFICATION CHANGED  
UNCLASSIFIED

**LIBRARY COPY**

JUN 23 1954

By authority of *72CH New Alt* *signature*  
*72-26* *Apr. 8, 1958*  
Date CLASSIFIED DOCUMENT

LANGLEY AERONAUTICAL LABORATORY  
LIBRARY, NACA  
HAMPTON, VIRGINIA

*HW 5-13-58*

This material contains information affecting the National Defense of the United States within the meaning of the espionage laws, Title 18, U.S.C., Secs. 793 and 794, the transmission or revelation of which in any manner to an unauthorized person is prohibited by law.

## NATIONAL ADVISORY COMMITTEE FOR AERONAUTICS

WASHINGTON

June 24, 1954

## NATIONAL ADVISORY COMMITTEE FOR AERONAUTICS

## RESEARCH MEMORANDUM

INVESTIGATION AT HIGH SUBSONIC SPEEDS OF THE EFFECT OF  
ADDING VARIOUS COMBINATIONS OF MISSILES ON THE  
AERODYNAMIC CHARACTERISTICS OF SWEEPBACK  
AND UNSWEPT WINGS COMBINED  
WITH A FUSELAGE

By H. Norman Silvers and William J. Alford, Jr.

## SUMMARY

An investigation was made at Mach numbers from 0.50 to 0.94 of the effects of two sizes of missiles in several combinations of spanwise and vertical positions on the aerodynamic characteristics of wing-fuselage combinations having a  $46.7^\circ$  sweptback wing and an essentially unswept wing ( $3.6^\circ$  sweepback).

The results of this investigation indicated that the installation drag of two small missiles was from 20 to 60 percent of the zero-lift drag of the wing-fuselage models and the installation drag of four small missiles was from 50 to 90 percent of the zero-lift drag of the swept-wing-fuselage model. Wing sweep had little apparent effect on the installation drag of comparable missile installations. Furthermore, the missile-installation drags were high compared with the installation drag of typical external-store installations. The installation-drag coefficients per unit of the installation total frontal area were from three to five times higher than the drag coefficients of the isolated missile. Although the installation drag per unit of installation total frontal area showed some reduction with increase in installation frontal area at Mach numbers around 0.75, there were no important changes in installation-drag coefficient with change in missile frontal area at Mach numbers around  $M = 0.92$ . Pylon length and missile spanwise location also had no major effect on the interference drag. The missile installations did not have any important effects on the lift or the stability characteristics of either the swept- or unswept-wing models.

## INTRODUCTION

The external carriage of air-launched missiles has brought about some new problems in connection with the performance of the launching airplane as well as the performance of the missile while in the presence of the airplane. To provide a better understanding of these problems, the National Advisory Committee for Aeronautics is conducting investigations of missiles on models both at low and at high speeds. This paper presents the results of an investigation of several typical missile arrangements on the aerodynamic characteristics at high subsonic speeds of wing-fuselage combinations having a  $46.7^\circ$  sweptback wing and a  $3.6^\circ$  sweptback wing. The results consist of lift, drag, and pitching-moment characteristics of the wing-fuselage combination alone and combined with the missiles.

## COEFFICIENTS AND SYMBOLS

$C_L$	lift coefficient, $\frac{\text{Lift}}{qS_w}$
$C_D$	drag coefficient, $\frac{\text{Drag}}{qS_w}$
$\Delta C_D$	drag due to lift, $C_D - C_{D_0}$
$C_{D_{m1}}$	drag coefficient of missile installation in terms of missile-body frontal area, $\left( C_{D_{\text{model+missile}}} - C_{D_{\text{model}}} \right) \frac{S_w}{nS_{m1}}$
$C_{D_{m2}}$	drag coefficient of missile installation in terms of total added frontal area of missile installation, $\left( C_{D_{\text{model+missile}}} - C_{D_{\text{model}}} \right) \frac{S_w}{nS_{m2}}$
$C_m$	pitching-moment coefficient referred to $0.25\bar{c}$ , $\frac{\text{Pitching moment}}{qS_w\bar{c}}$
$S_w$	wing area, sq ft
$S_{m1}$	frontal area of missile body, sq ft
$S_{m2}$	total added frontal area of missile installation, including body, fins, and pylon, sq ft

n number of missiles

$\bar{c}$  mean aerodynamic chord of wing,  $\frac{2}{S_w} \int_0^{b/2} c^2 dy$ , ft

l length of body

q dynamic pressure,  $\frac{\rho V^2}{2}$ , lb/sq ft

$\rho$  air density, slugs/cu ft

V airstream velocity, ft/sec

M Mach number

R Reynolds number of wing based on  $\bar{c}$

$\alpha$  angle of attack, deg

$$C_{L\alpha} = \left( \frac{\partial C_L}{\partial \alpha} \right)_M$$

$$C_{mC_L} = \left( \frac{\partial C_m}{\partial C_L} \right)_M$$

Subscripts:

f fuselage

m missile

o zero lift

#### MODELS AND APPARATUS

The test vehicles consisted of a fuselage equipped in turn with wings - one swept back  $46.7^\circ$ , referred to hereafter as the swept wing, and the other swept back  $3.6^\circ$ , referred to hereafter as the unswept wing. The wings were constructed of aluminum and were of aspect ratio 4.0, taper ratio 0.6, and had NACA 65A006 airfoil sections parallel to the plane of symmetry of the model. The fuselage contour was made up of parabolic-arc segments, the ordinates of which are presented in table I. The arrangements of the wings on the fuselage and the missiles on the

wings are shown in figures 1 and 2. A photograph of the swept-wing model with one arrangement of the missiles is presented in figure 3.

The missiles were suspended from the wings in all test installations by 6-percent-thick, flat-sided pylons (ordinates presented in fig. 4). The missile-installation variables were missile spanwise location, missile size, and pylon length. The missile spanwise locations used were  $0.33b/2$  and  $0.487b/2$ . Two sizes of missiles were investigated. The smaller missile as mounted on the test vehicle was considered representative of this type missile mounted on a full-scale, fighter-type airplane. Of the two pylon lengths investigated, the shorter length was designed to provide a  $1/16$ -inch gap between the lower surface of the wing of the wing-fuselage model and the tips of the wings of the small missile. The longer pylon when used with the large missile also provided a  $1/16$ -inch gap between the missile wing tips and the lower surface of the wing of the wing-fuselage model. Detail dimensions of the missile installations and the pylon geometry are presented in figure 4. The general proportions of the missile are shown in figure 5.

The primary test vehicle was the sweptback-wing—fuselage model. The various combinations of missile location, size, and length of pylon support that were investigated on the sweptback-wing model, as well as those investigated on the unswept-wing model to determine the importance of wing sweep, are summarized in table II.

The wing-fuselage models were attached to the support sting by a strain-gage balance. Forces and moments of the wing-fuselage models with and without missiles were indicated by galvanometer deflections that were automatically recorded during all tests.

## TESTS

The tests were made in the Langley high-speed 7- by 10-foot tunnel at Mach numbers ranging from 0.50 to about 0.94 over an angle-of-attack range that extended from  $-2^\circ$  to a maximum of  $24^\circ$  at the lower Mach numbers. At the higher Mach numbers the maximum angle of attack was restricted by the model loading conditions. Two types of tests were made. In one type, tests were made in which lift, drag, and pitching-moment results were obtained through the angle-of-attack range at a constant Mach number. In the other type, tests were made at zero lift of the model through the Mach number range in order to measure the zero-lift drag characteristics with a maximum of accuracy.

For the zero-lift drag runs through the Mach number range, the accuracy levels of the drag coefficients are indicated in the following table:

M	Accuracy in $C_D$	Accuracy in $C_{D_{m1}}$	
		One small missile	Four small missiles
0.50	$\pm 0.0007$	$\pm 0.70$	$\pm 0.17$
.60	$\pm 0.0005$	$\pm .52$	$\pm .13$
.70	$\pm 0.0004$	$\pm .41$	$\pm .10$
.80	$\pm 0.0004$	$\pm .35$	$\pm .09$
.90	$\pm 0.0003$	$\pm .30$	$\pm .08$
.94	$\pm 0.0003$	$\pm .29$	$\pm .07$

where values of  $C_D$  are based on wing area and values of  $C_{D_{m1}}$  are based on frontal areas of the missile bodies.

The table shows that, as the total missile frontal area increases, the accuracy of the missile-installation drag in coefficient form increases.

The variation in Reynolds number with Mach number of this investigation is presented in figure 6.

#### CORRECTIONS

Blocking corrections applied to Mach number and dynamic pressure were determined by the velocity-ratio method of reference 1, which utilizes experimental pressures measured at the tunnel wall opposite the model. Over the Mach number range investigated, good agreement was obtained between these corrections and those obtained theoretically by the method of reference 2.

The jet-boundary corrections applied to the angle of attack and drag of the complete model were obtained by the method of reference 3. Corrections to the pitching moment were considered negligible. No support tares have been applied as they are believed to be small.

Drag data have been corrected to correspond to a pressure at the base of the fuselage equal to free-stream static pressure. Base pressure was determined by measuring the pressure at a point inside the fuselage about 9 inches forward of the base. This correction, which was added to the measured drag coefficient, amounted to 0.0010 at  $M = 0.80$  and increased to 0.0030 at  $M = 0.91$ . As indicated in reference 4, external stores

have essentially no effect on fuselage base pressure. A buoyancy correction which resulted from the static-pressure gradient that exists along the tunnel center line - determined from static-pressure surveys - was added to the drag results of this paper. The increment in drag coefficient due to buoyancy amounted to 0.0016 throughout the Mach number range.

Corrections have been applied to the angle of attack to account for deflection of the support system under load. No correction has, however, been applied to the results presented in this paper to account for aeroelasticity of the wing.

## RESULTS AND DISCUSSION

### Presentation of Results

The results of the investigation are presented in the following figures:

	Figure
Basic-data:	
Swept-wing model . . . . .	7
Swept-wing model with missiles . . . . .	8
Unswep-wing model . . . . .	9
Unswep-wing model with missiles . . . . .	10
Summary data:	
Variation of $C_D$ with $M$ . . . . .	11
Variation of $C_{Dm}$ with $S_m/S_w$ . . . . .	12
Variation of $\Delta C_D$ with $C_L$ . . . . .	13
Variation of $C_{L\alpha}$ with $M$ . . . . .	14
Variation of $C_{mC_L}$ with $M$ . . . . .	15

Lift-curve and pitching-moment-curve slopes were measured at zero angle of attack and zero lift coefficient, respectively.

### Drag Characteristics

The drag characteristics at zero lift of the models with and without the various missile installations are shown in figure 11. For configurations involving two of the smaller missiles on either the unswept or the swept back wing (configurations B, C, F, J, and L), the drag increment attributable to the missile installation ranged from about 20 percent to 60 percent of the zero-lift drag of the clean wing-fuselage models for Mach numbers below 0.92. Four small missiles (configuration A), which

were investigated on the swept-wing model, caused a drag increase of from 50 to 90 percent in the drag of the clean wing-fuselage model at Mach numbers below 0.92 (fig. 11(a)). Four missiles, which is a normal complement of missiles, obviously produce drag levels that would impose severe penalties to the performance of high-speed fighters.

Below drag-rise Mach number, wing sweep did not have any appreciable effect on the drag contribution of comparable missile installations (fig. 11).

There are several ways to reduce the installation drag to a coefficient form that is related to the geometry of the installation. In the present paper, two types of installation-drag coefficient are presented; first, installation drag is based on missile body frontal area and called  $C_{D_{m_1}}$  and, second, it is based on the total frontal area of the installation including the frontal areas of missile bodies, pylons, and missile wings and called  $C_{D_{m_2}}$ . The installation-drag coefficients are summarized

in figures 12(a) and 12(b) as a function of the ratio of missile reference frontal area to the model wing area. It is common practice in external store and nacelle work to use only the frontal area of the store or nacelle as the area basis for drag coefficients (equivalent to  $C_{D_{m_1}}$ ).

Comparison of the missile installation-drag coefficients with the drag coefficients of typical external-store arrangements (refs. 4 and 5 and unpublished data of fig 12(a)) shows that the drag of the missile installations is several times that of the stores. Although the stores are larger than the missiles they do not have interference-producing forward wings. The total interference drag of the missile installation can be obtained by comparison of the results with the drag coefficients of the isolated missile, results for which were obtained from unpublished data. Perhaps the more suitable indication of the installation interference can be obtained from the drag coefficient  $C_{D_{m_2}}$  (fig. 12(b)) because it

is based on the frontal areas of all of the components of installation that contribute to the interference. Excluding the results on the unswept-wing model at  $M = 0.92$  which are well beyond drag rise of the model, the interference drag appears to be from three to five times the drag of the isolated missiles. This order of magnitude of interference drag is excessive. One point of interest shown in figure 12(b) at  $M = 0.75$  is that the installation-drag coefficient per unit of total installation frontal area shows some reduction as the frontal area of the installation is increased. Larger reductions with increase in installation reference area and at both Mach numbers are shown in figure 12(a). The magnitude of the reductions in  $C_{D_{m_1}}$  appears to be more a result of the choice of areas

rather than an interference effect. In fact, at  $M = 0.92$   $C_{D_{m_2}}$

(fig. 12(b)) and hence the interference appears to be independent of installation frontal area on the swept-wing model. The results also show that changes in pylon length and missile spanwise location had no important effects on  $C_{D_{m_2}}$  at either  $M = 0.75$  or  $M = 0.92$  on the swept-wing model.

Shown in figures 13(a) and 13(b) are the increments in total drag coefficient that result from an increase in lift coefficient of the models. The solid curves represent the change in drag due to lift of models without missiles and the hatched areas between the other curves represent the changes in drag due to lift that come from the various arrangements of the missiles. The results indicate that increase in lift coefficient did not produce any major changes in the drag characteristics of the missile installations.

#### Lift and Pitch Characteristics

The effects of the various missile arrangements on the lift-curve and pitching-moment-curve slopes are presented in figures 14 and 15. The maximum changes in these parameters due to change in the missile installation configuration are designated by the hatched regions. It is apparent from these results that the presence of any of the missile installations had no important effects on the characteristics considered, except in the case of the unswept-wing model at the highest Mach numbers. At these speeds, missile installations tend to reduce the lift-curve slopes and tend to minimize the rapid changes with Mach number of the location of the aerodynamic center.

#### CONCLUSIONS

An investigation at high subsonic speeds of the effect of missiles on the aerodynamic characteristics of a sweptback wing and an unswept wing combined with a fuselage indicate the following conclusions:

1. The installation drags of two small missiles were from 20 to 60 percent of the zero-lift drag of the wing-fuselage models and the installation drags of four small missiles were from 50 to 90 percent of the zero-lift drag of the swept-wing-fuselage model. Wing sweep had little apparent effect on the installation drag of comparable missile installations. Furthermore, the missile-installation drags were high compared with the installation drag of typical external-store installations.

2. The installation-drag coefficient per unit of the installation total frontal area was from three to five times higher than the drag coefficient of the isolated missile. Although the installation drag per unit of installation total frontal area showed some reduction with increase in installation frontal area at Mach numbers around 0.75, there were no important changes in installation-drag coefficient with change in missile frontal area at Mach numbers around 0.92. Pylon length and missile spanwise location also had no major effect on the interference drag.

3. The missile installations had no important effects on the lift or the stability characteristics of either the swept- or unswept-wing models.

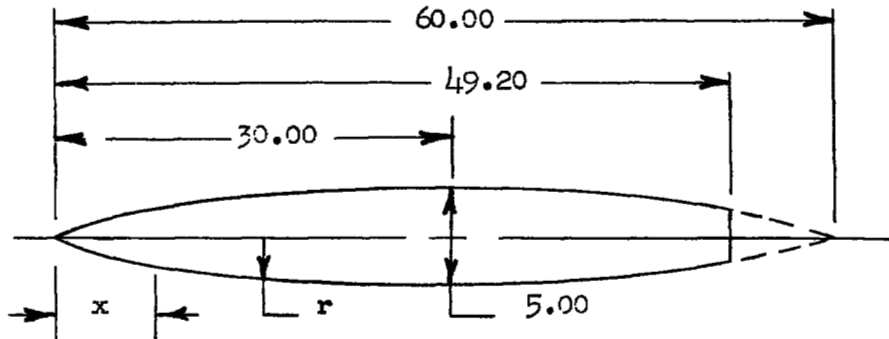
Langley Aeronautical Laboratory,  
National Advisory Committee for Aeronautics,  
Langley Field, Va., April 7, 1954.

#### REFERENCES

1. Hensel, Rudolph W.: Rectangular-Wind-Tunnel Blocking Corrections Using the Velocity-Ratio Method. NACA TN 2372, 1951.
2. Herriot, John G.: Blockage Corrections for Three-Dimensional-Flow Closed-Throat Wind Tunnels, With Consideration of the Effect of Compressibility. NACA Rep. 995, 1950. (Supersedes NACA RM A7B28.)
3. Gillis, Clarence L., Polhamus, Edward C., and Gray, Joseph L., Jr.: Charts for Determining Jet-Boundary Corrections for Complete Models in 7- by 10-Foot Closed Rectangular Wind Tunnels. NACA WR L-123, 1945. (Formerly NACA ARR L5G31.)
4. Silvers, H. Norman, and King, Thomas J., Jr.: Investigation at High Subsonic Speeds of Bodies Mounted From the Wing of an Unswept-Wing - Fuselage Model, Including Measurements of Body Loads. NACA RM L52J08, 1952.
5. Silvers, H. Norman, and King, Thomas J., Jr.: A Small-Scale Investigation of the Effect of Spanwise and Chordwise Positioning of an Ogive-Cylinder Underwing Nacelle on the High-Speed Aerodynamic Characteristics of a  $45^\circ$  Sweptback Tapered-in-Thickness Wing of Aspect Ratio 6. NACA RM L52J22, 1952.

TABLE I  
FUSELAGE ORDINATES

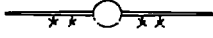
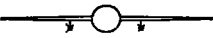
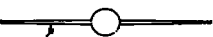
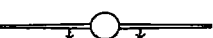
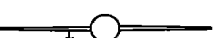
[Basic fineness ratio 12; actual fineness ratio 9.8 achieved  
by cutting off rear portion of body]



Ordinates, in.	
x	r
0	0
.30	.139
.45	.179
.75	.257
1.50	.433
3.00	.723
4.50	.968
6.00	1.183
9.00	1.556
12.00	1.854
15.00	2.079
18.00	2.245
21.00	2.360
24.00	2.438
27.00	2.486
30.00	2.500
33.00	2.478
36.00	2.414
39.00	2.305
42.00	2.137
49.20	1.650

L.E. radius = 0.030 in.

*Table II*  
*Summary of Missile Installations*

<i>Model</i>	<i>Missile config.</i>	<i>Wing sweep</i>	<i>Missile size</i>	<i>Pylon length</i>	<i>Installation drag at M=0.75</i>	
					$\Delta C_D$	$C_{Dm}$
	<i>A</i>	<i>46.7°</i>	<i>Small</i>	<i>Short</i>	<i>.0053</i>	<i>1.34</i>
	<i>B</i>	<i>-do-</i>	<i>-do-</i>	<i>-do-</i>	<i>.0031</i>	<i>1.57</i>
	<i>C</i>	<i>-do-</i>	<i>-do-</i>	<i>-do-</i>	<i>.0029</i>	<i>1.47</i>
	<i>D</i>	<i>-do-</i>	<i>-do-</i>	<i>-do-</i>	<i>.0024</i>	<i>2.48</i>
	<i>E</i>	<i>-do-</i>	<i>-do-</i>	<i>-do-</i>	<i>.0016</i>	<i>1.62</i>
	<i>F</i>	<i>-do-</i>	<i>-do-</i>	<i>Long</i>	<i>.0034</i>	<i>1.72</i>
	<i>G</i>	<i>-do-</i>	<i>-do-</i>	<i>-do-</i>	<i>.0022</i>	<i>2.23</i>
	<i>H</i>	<i>-do-</i>	<i>Large</i>	<i>-do-</i>	<i>.0054</i>	<i>0.95</i>
	<i>I</i>	<i>-do-</i>	<i>-do-</i>	<i>-do-</i>	<i>.0034</i>	<i>1.21</i>
	<i>J</i>	<i>3.6°</i>	<i>Small</i>	<i>Short</i>	<i>.0031</i>	<i>1.57</i>
	<i>K</i>	<i>-do-</i>	<i>-do-</i>	<i>-do-</i>	<i>.0015</i>	<i>1.52</i>
	<i>L</i>	<i>-do-</i>	<i>-do-</i>	<i>Long</i>	<i>.0040</i>	<i>2.03</i>

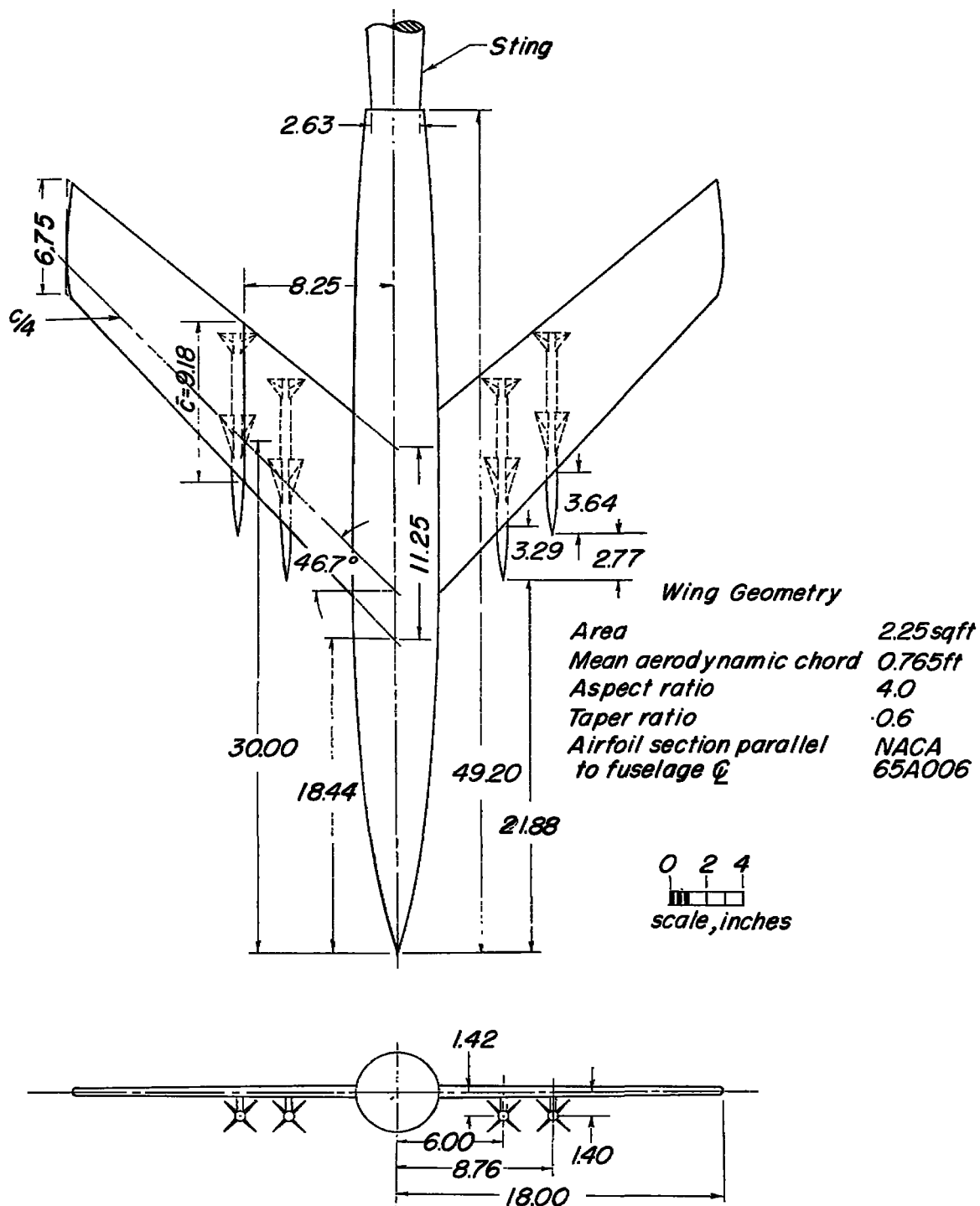


Figure 1.- Drawing of the swept-wing model.

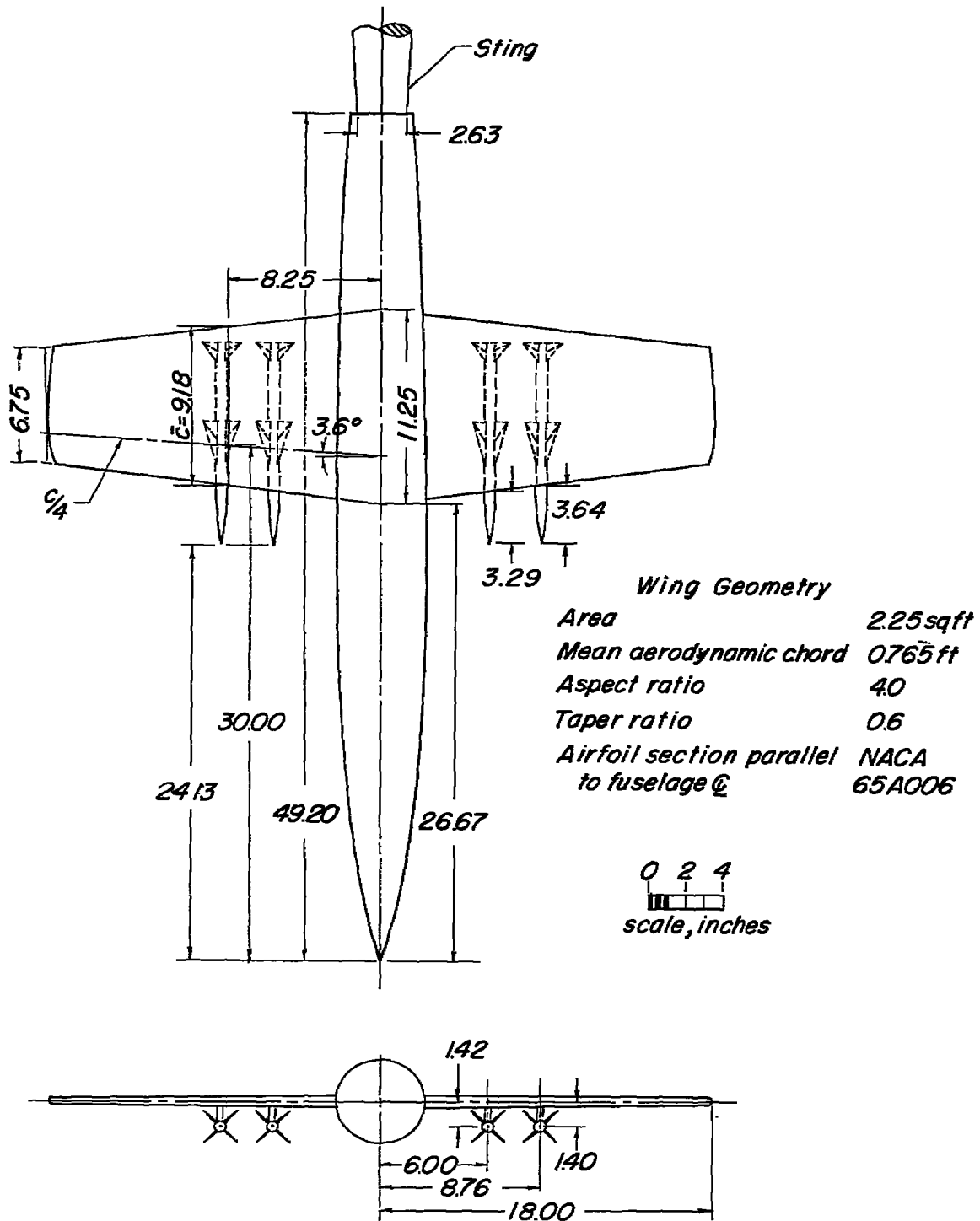
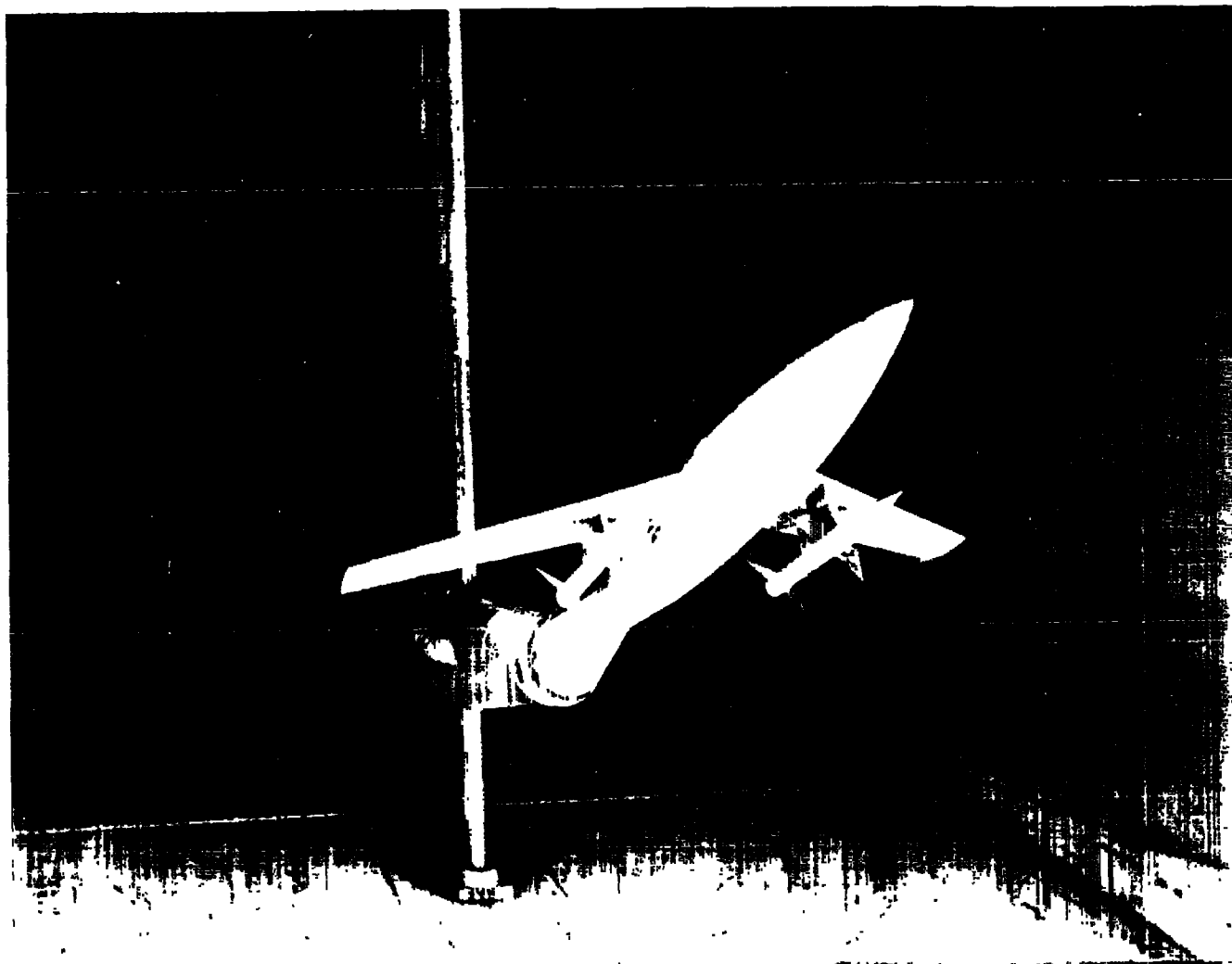


Figure 2.- Drawing of the unswept-wing model.



L-77773

Figure 3.- Photograph of the test setup in the Langley high-speed  
7- by 10-foot tunnel.

Missile	Pylon	Z		Frontal areas, sq in.	
		inboard	outboard	$S_{m_1}$	$S_{m_2}$ (inb.=outb.)
small	short	1.42	1.40	0.330	0.765
small	long	1.92	1.90	0.330	0.950
large	long	2.13	—	0.915	1.780

$S_{m_1}$  - frontal area of one missile body

$S_{m_2}$  - frontal area of one missile body + pylon + missile wings.

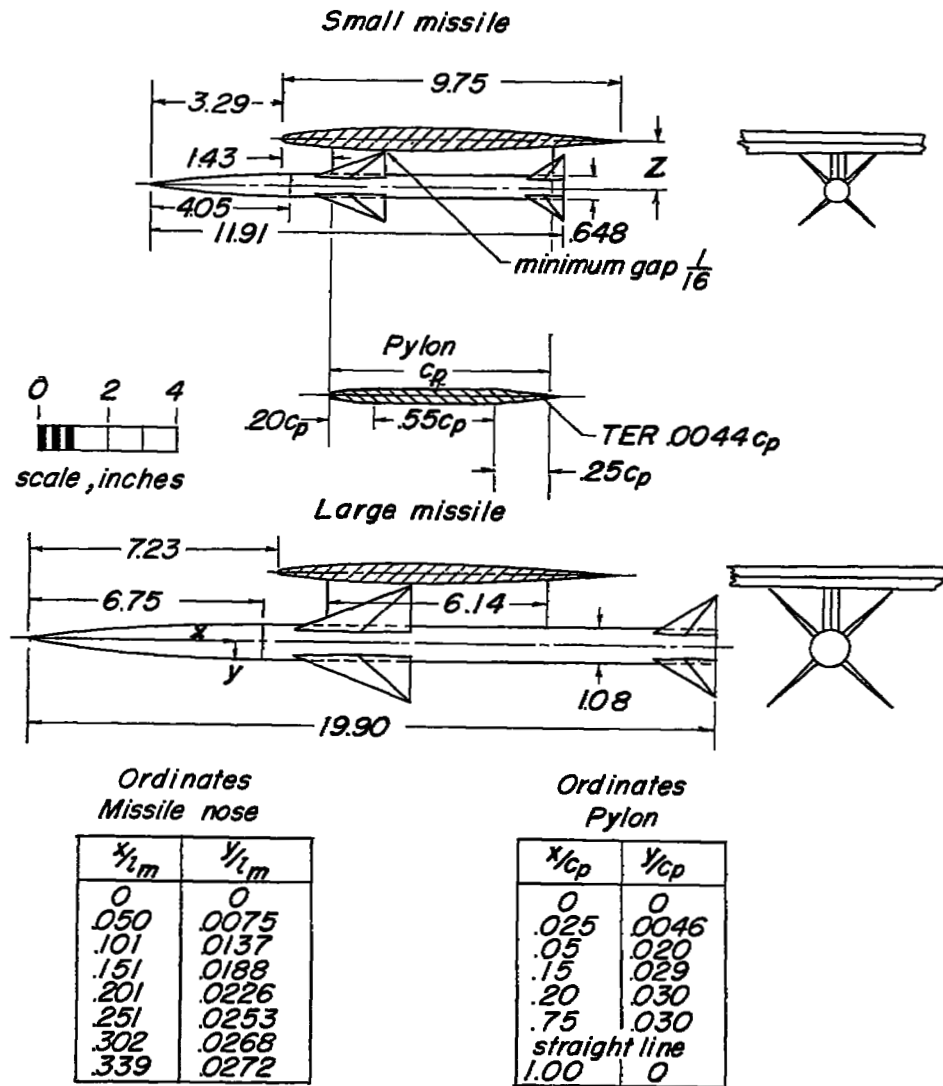


Figure 4.- Drawings of the missile models in the inboard location.

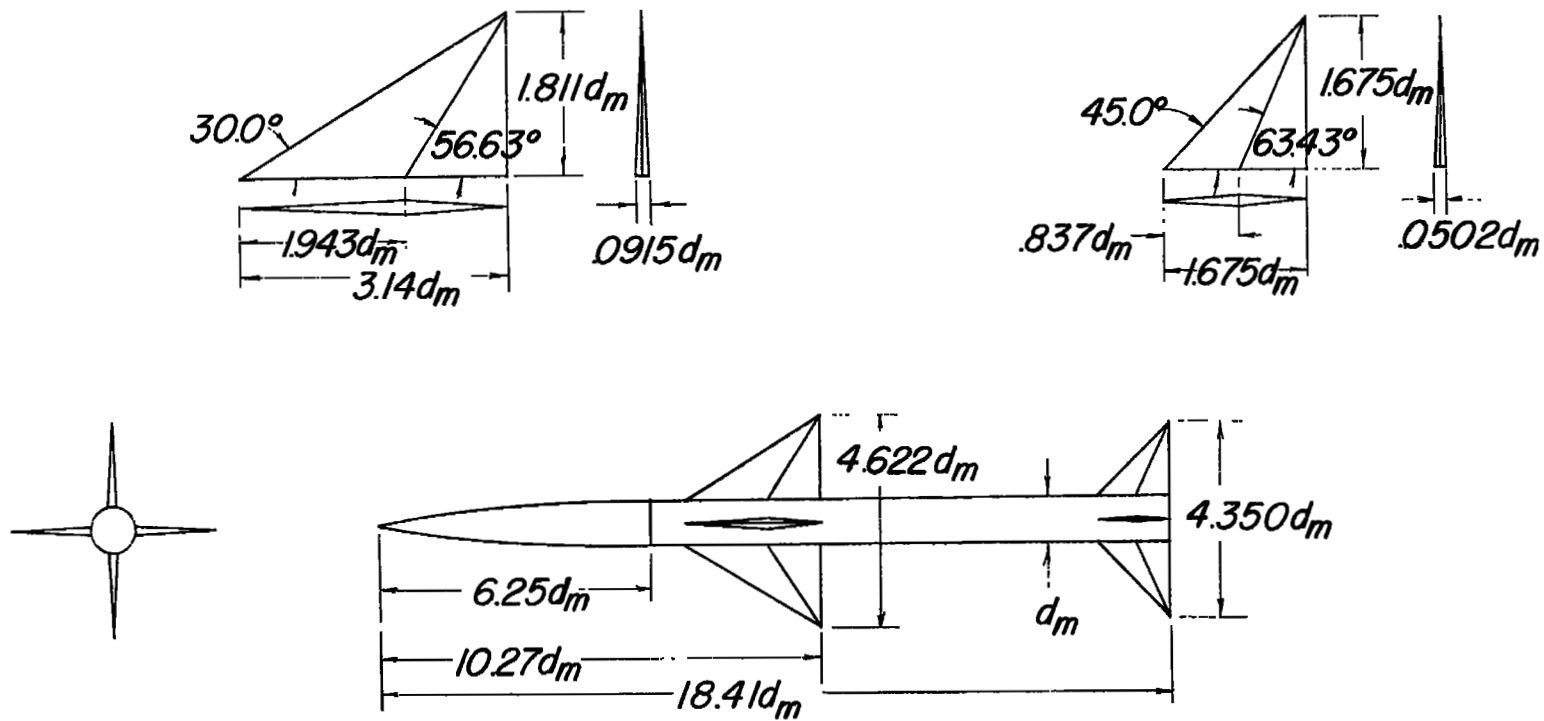


Figure 5.- Drawing of the missile model showing general proportions.

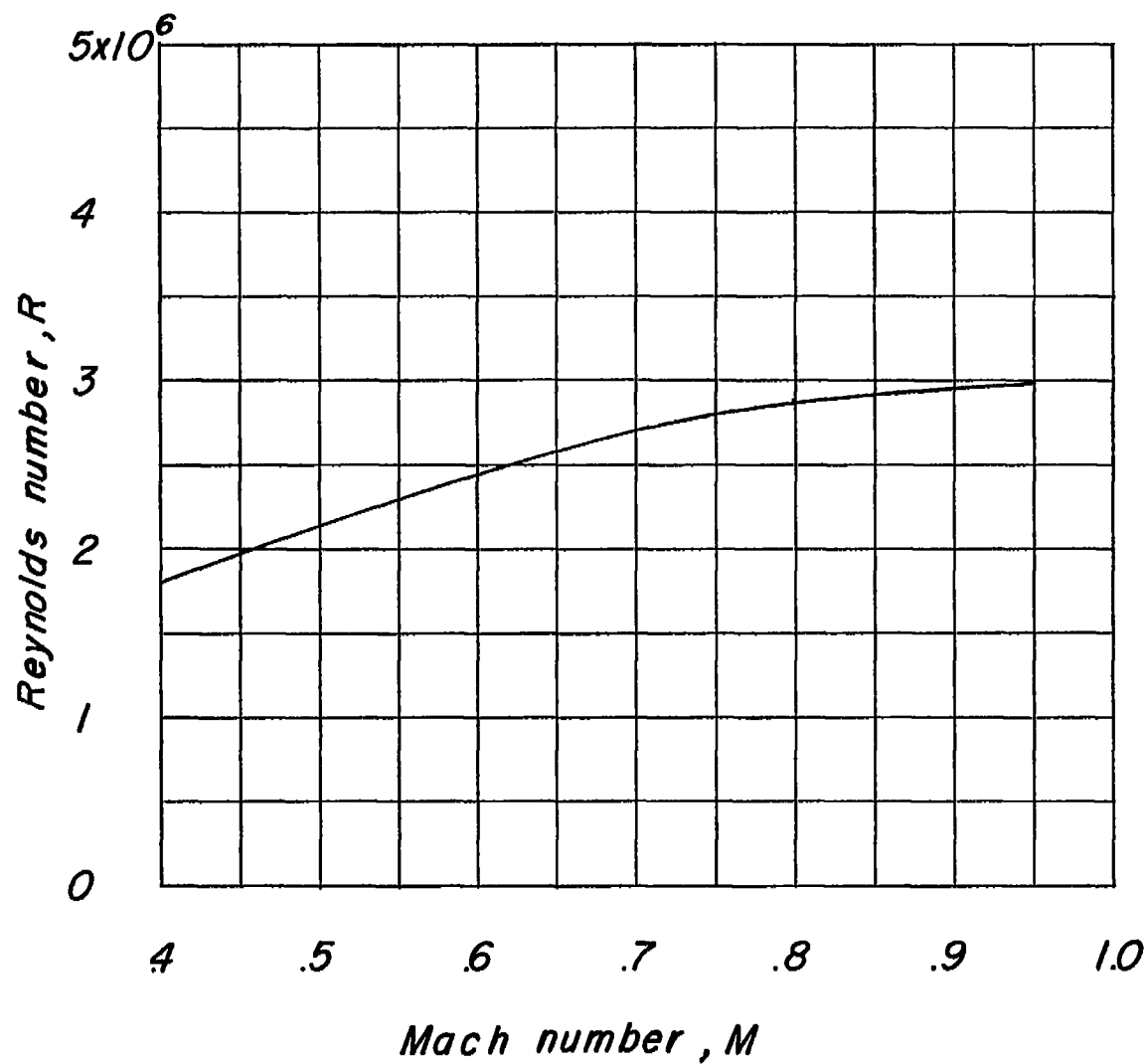


Figure 6.- Variation with Mach number of mean test Reynolds number based on the wing mean aerodynamic chord of 0.765 foot.

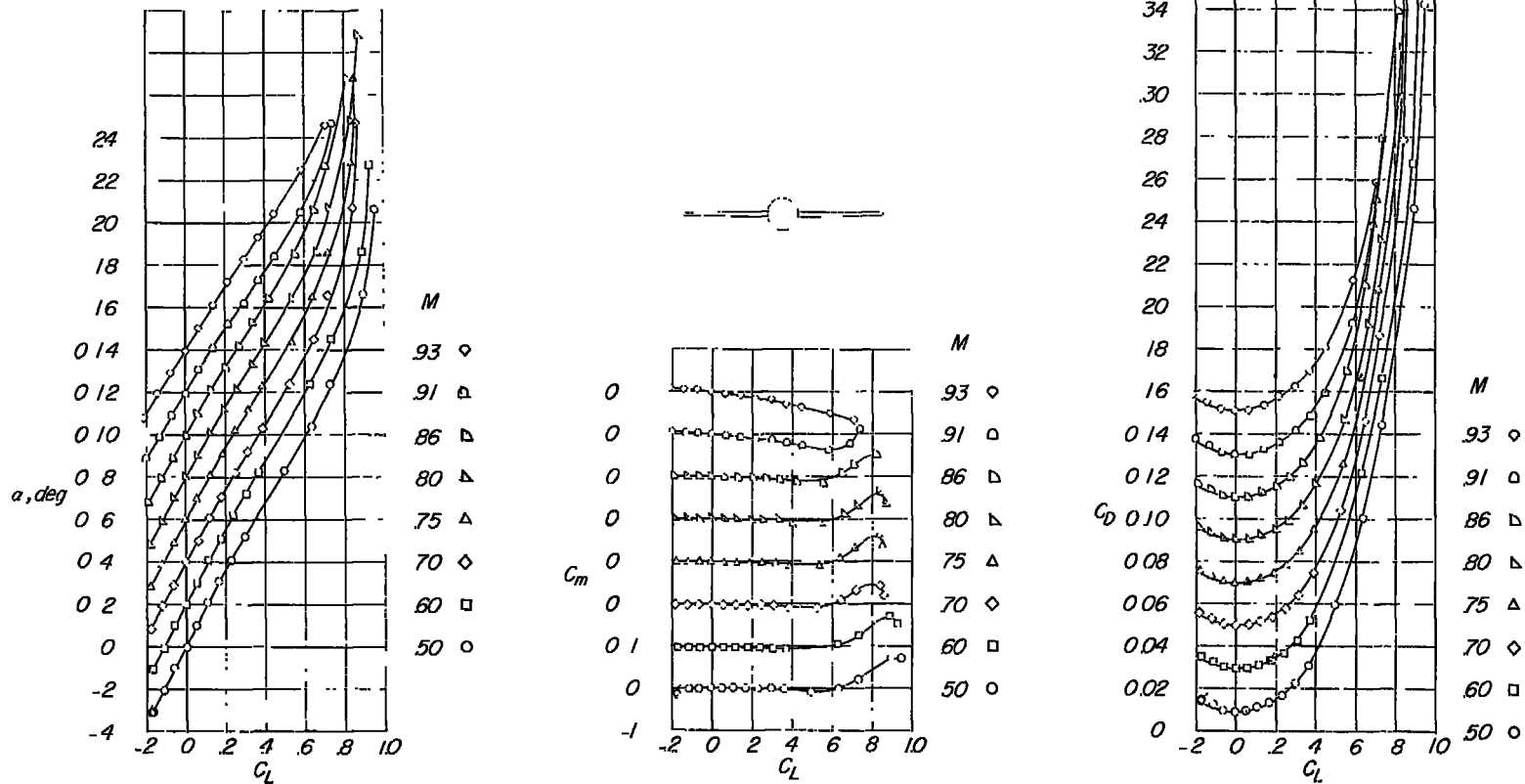
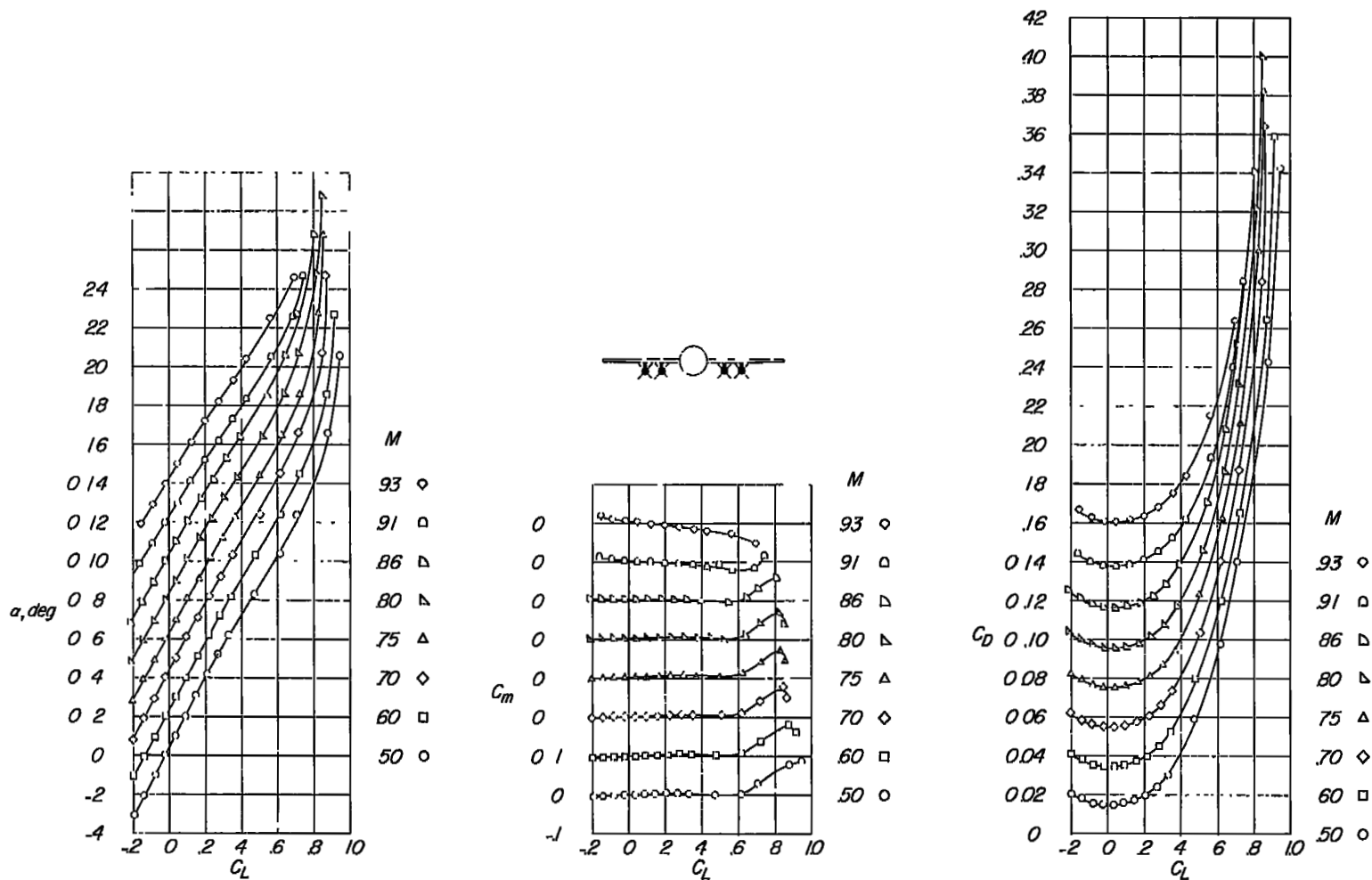
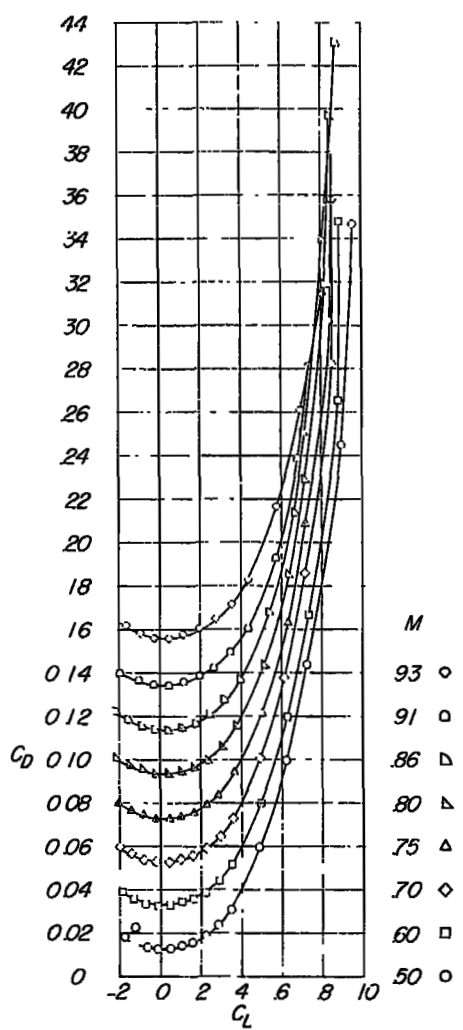
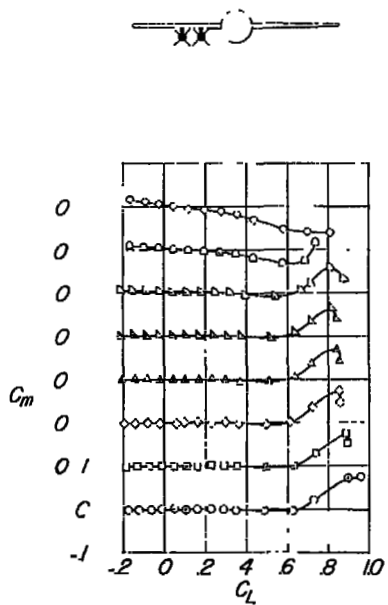
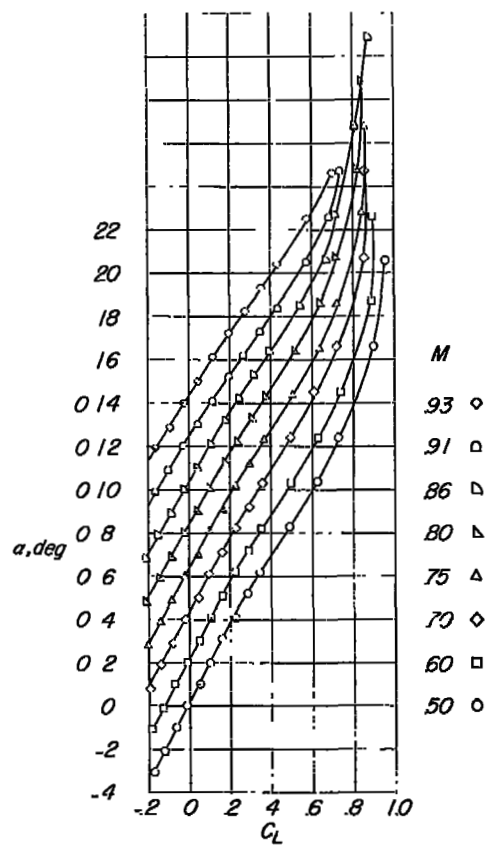


Figure 7.- Aerodynamic characteristics of the 46.7° sweptback-wing-fuselage combination.



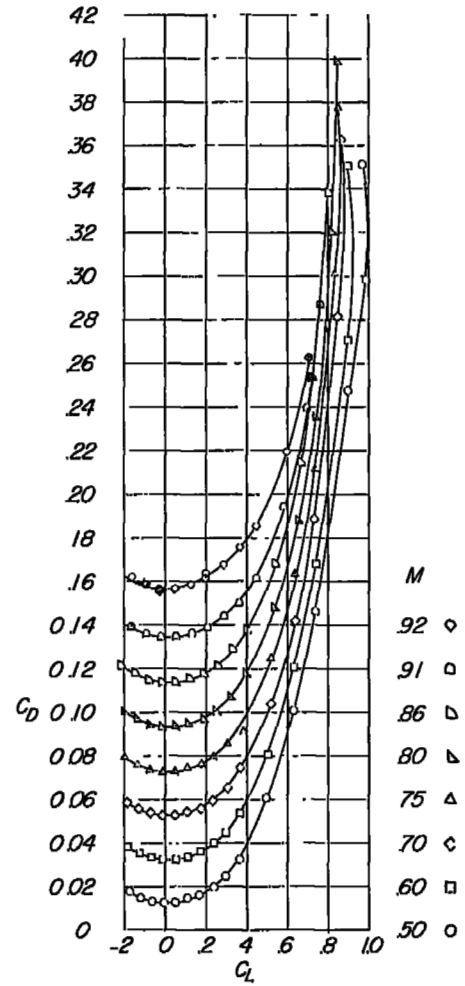
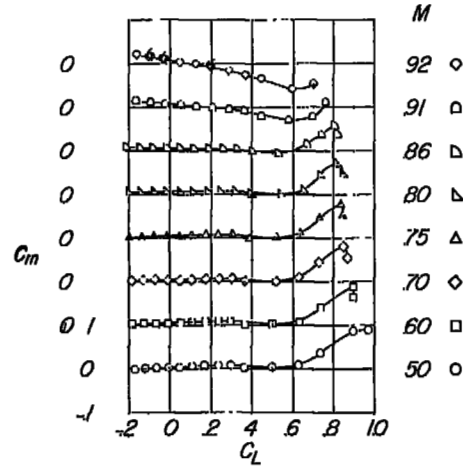
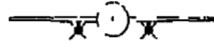
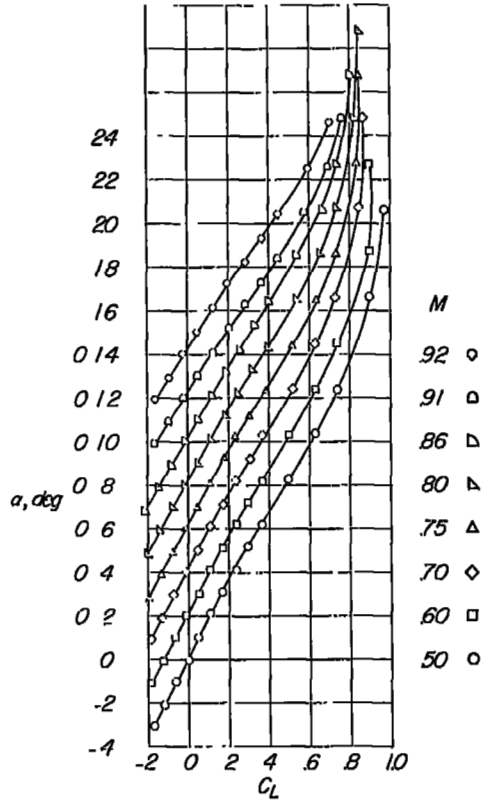
(a) Missile configuration A.

Figure 8.- Aerodynamic characteristics of the 46.7° sweptback-wing-fuselage model with the various configurations of the missiles.



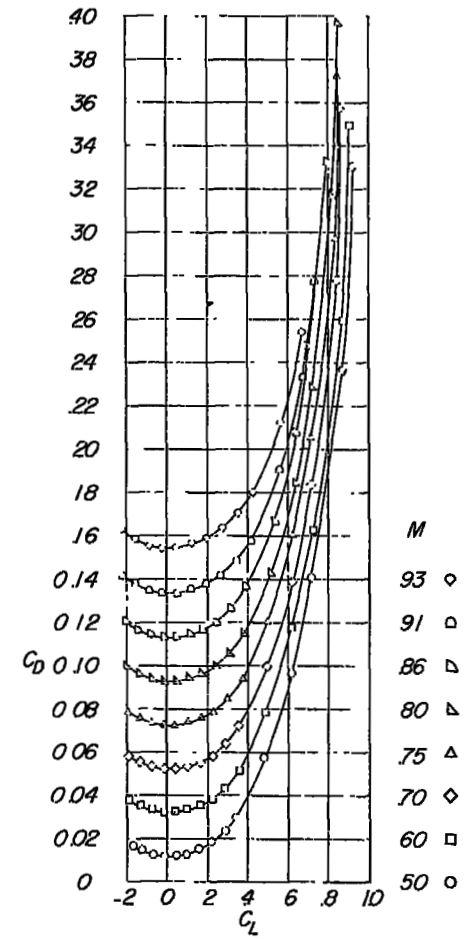
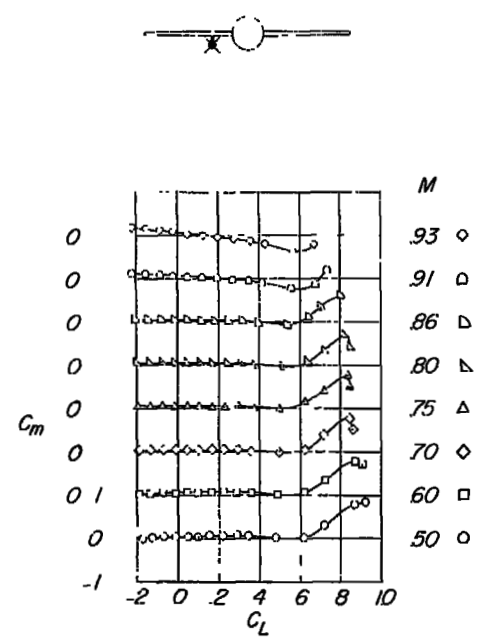
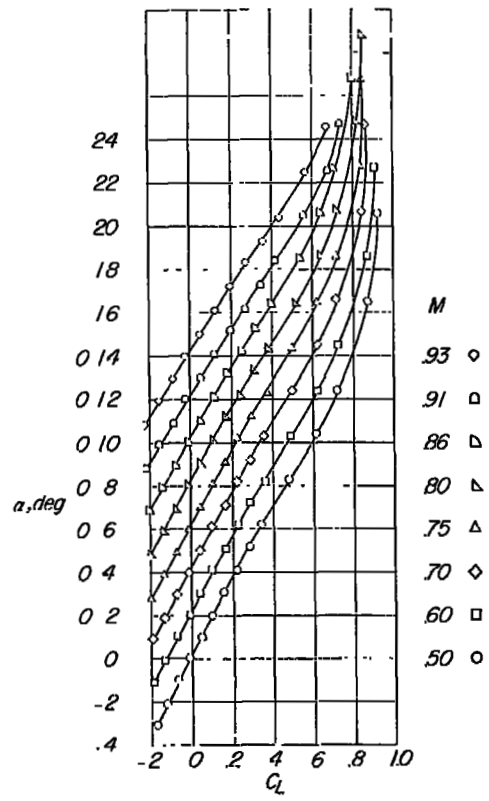
(b) Missile configuration B.

Figure 8.- Continued.



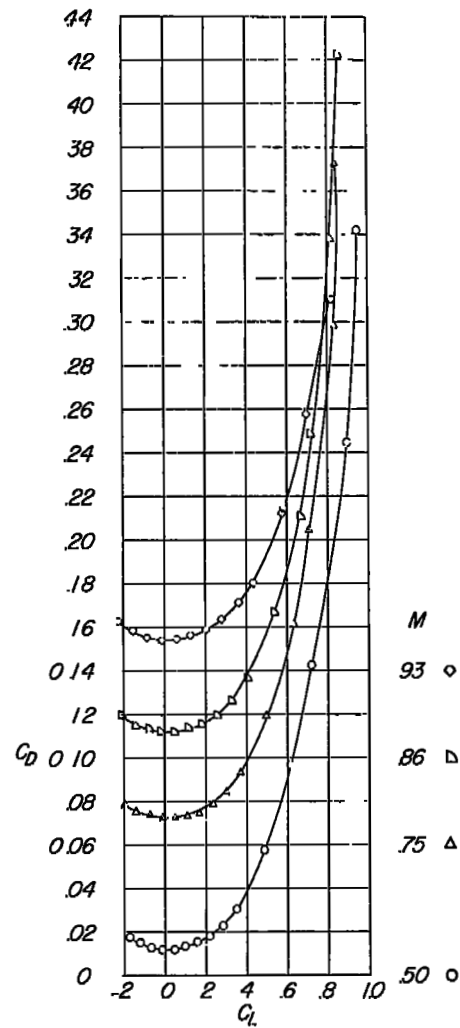
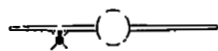
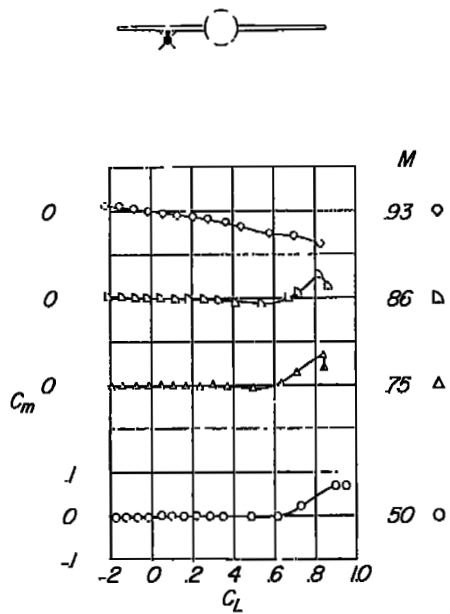
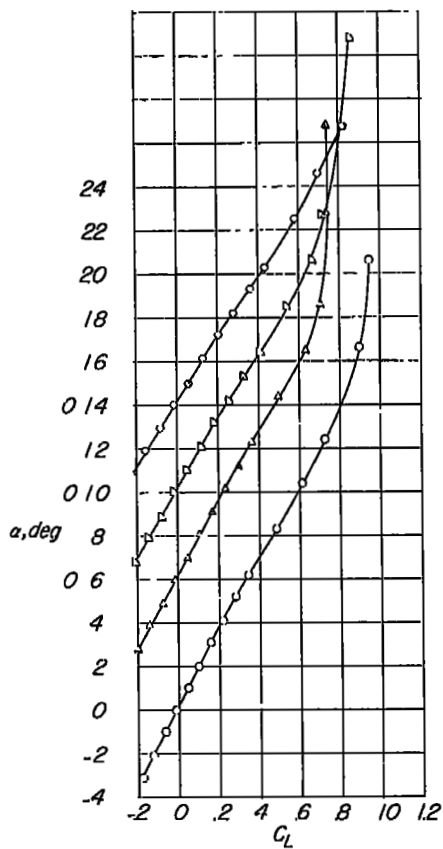
(c) Missile configuration C.

Figure 8.- Continued.



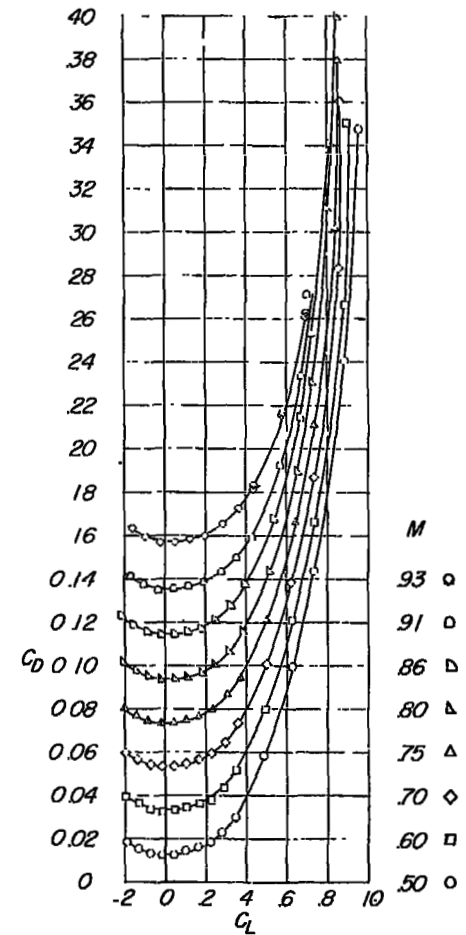
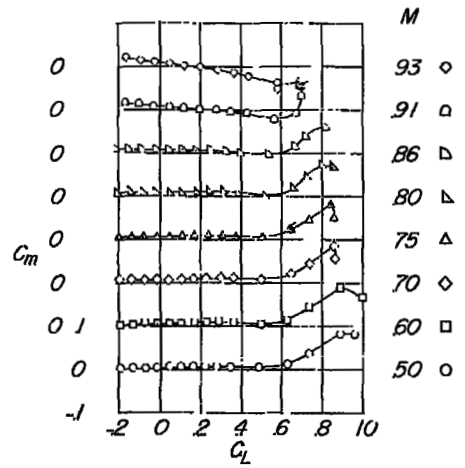
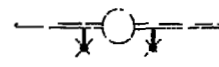
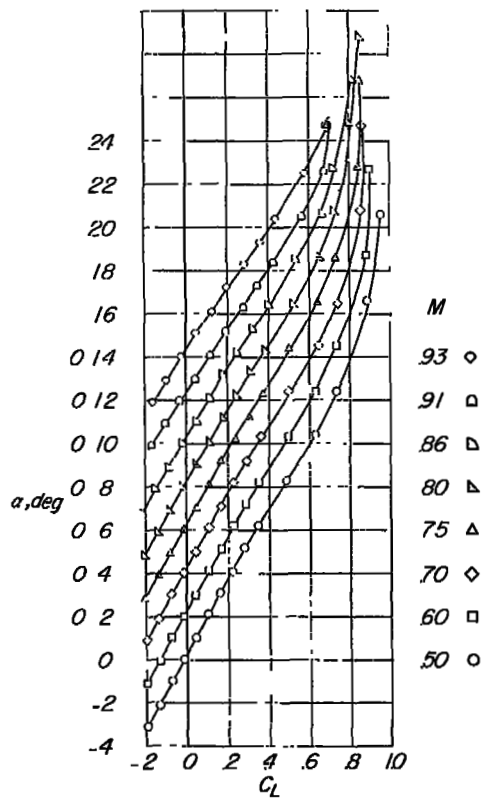
(d) Missile configuration D.

Figure 8.- Continued.



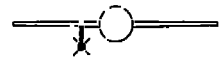
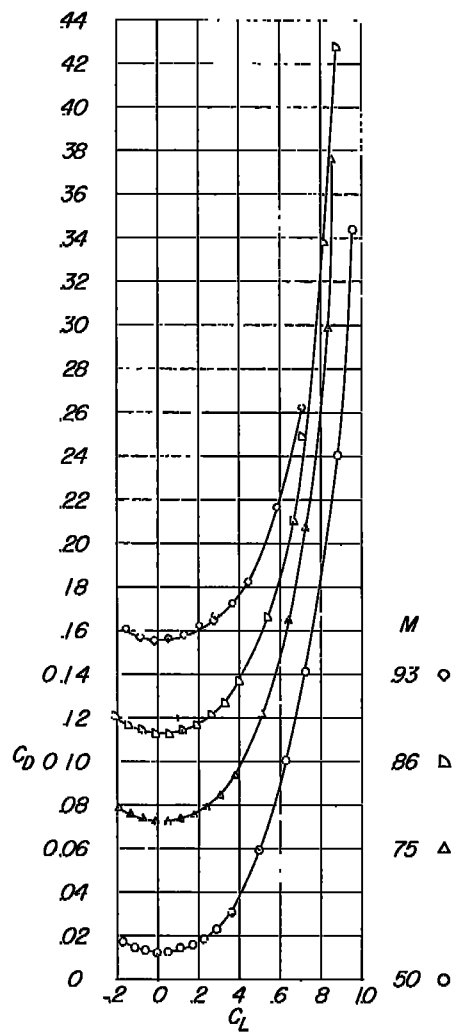
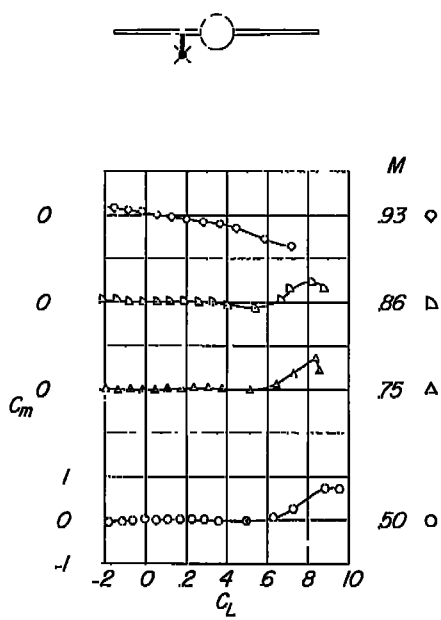
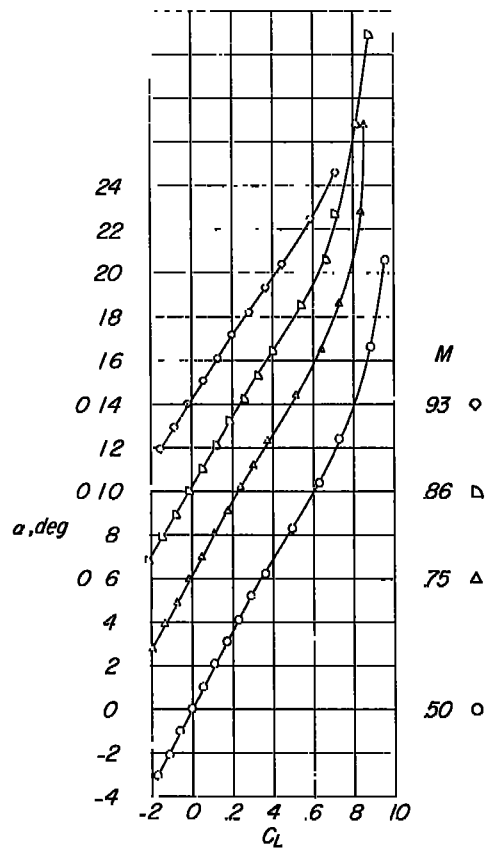
(e) Missile configuration E.

Figure 8.- Continued.



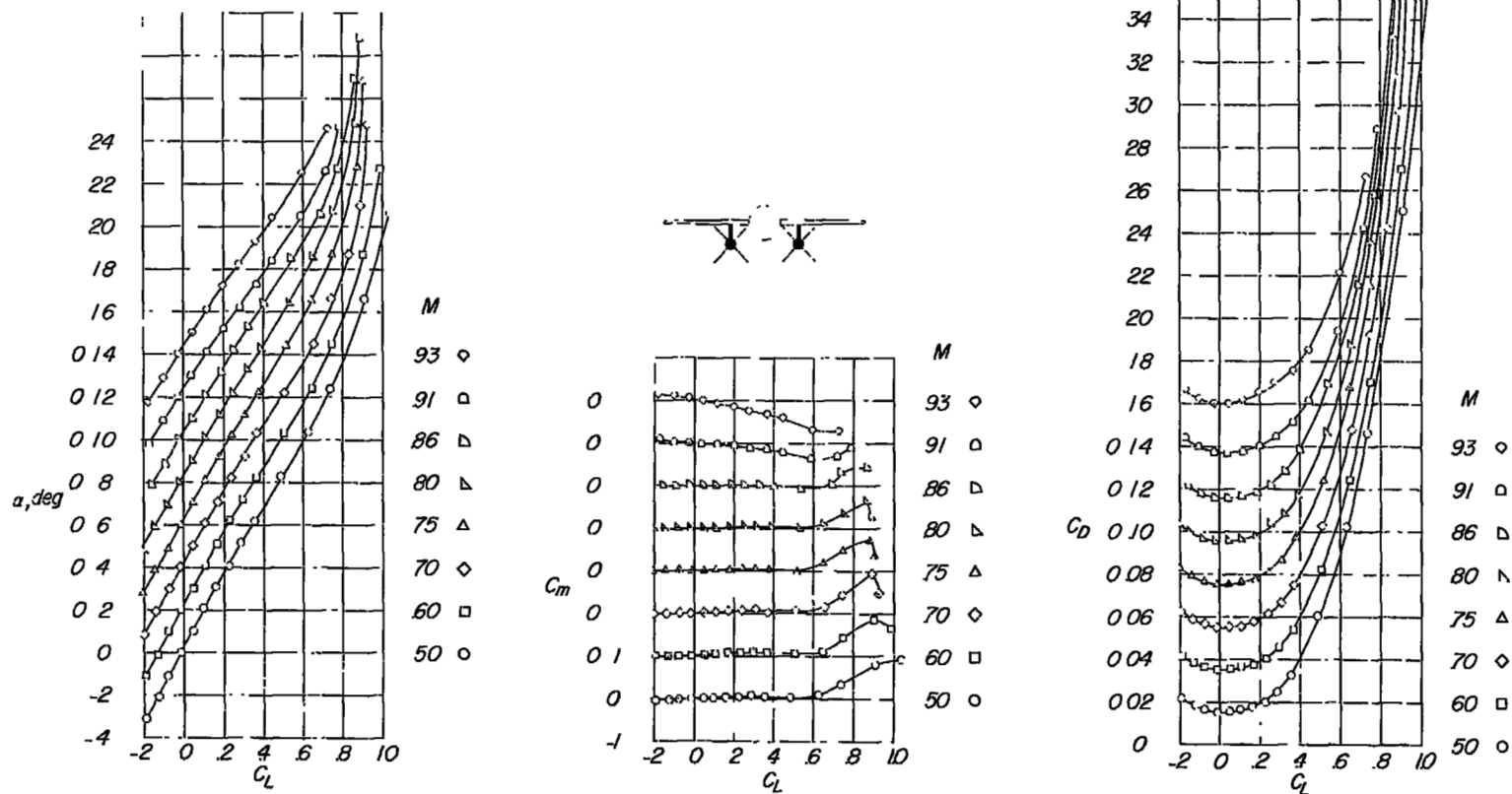
(f) Missile configuration F.

Figure 8.- Continued.



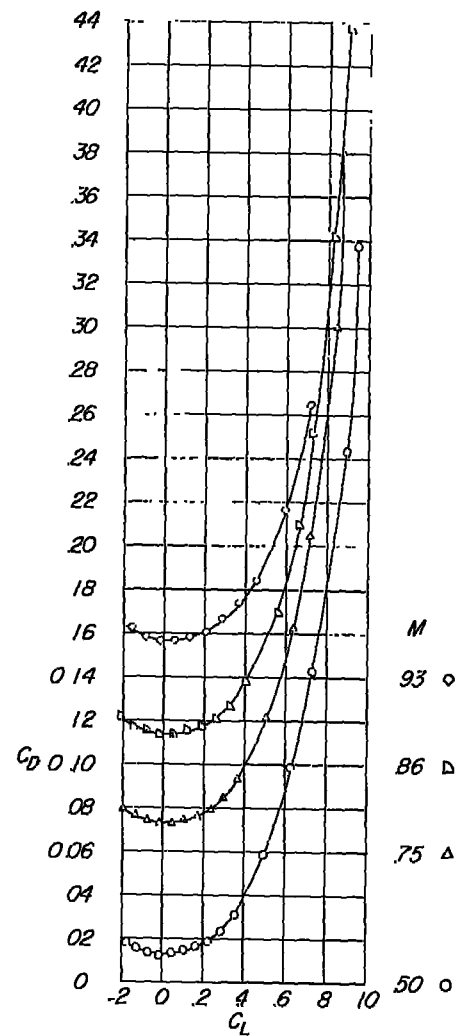
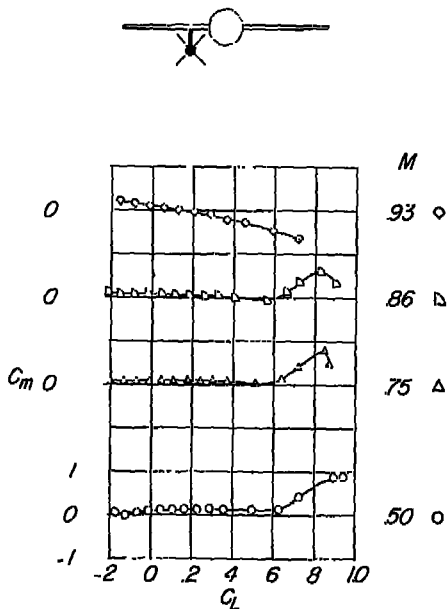
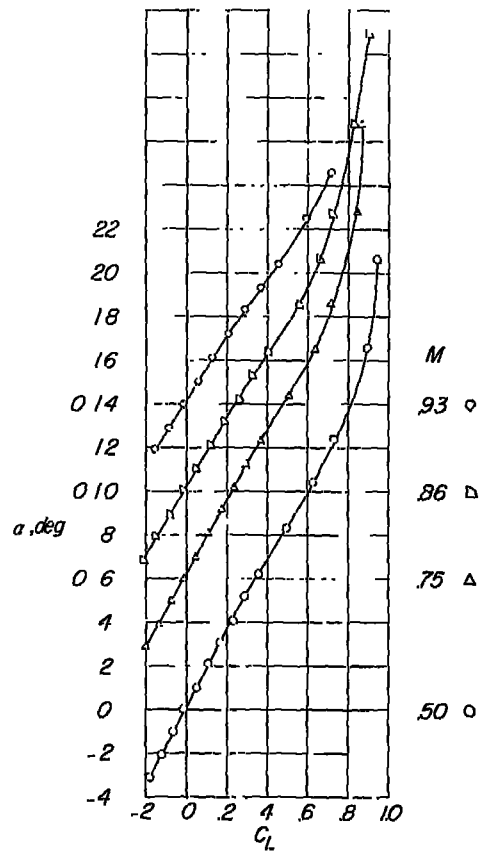
(g) Missile configuration G.

Figure 8.- Continued.



(h) Missile configuration H.

Figure 8.- Continued.



(i) Missile configuration I.

Figure 8.- Concluded.

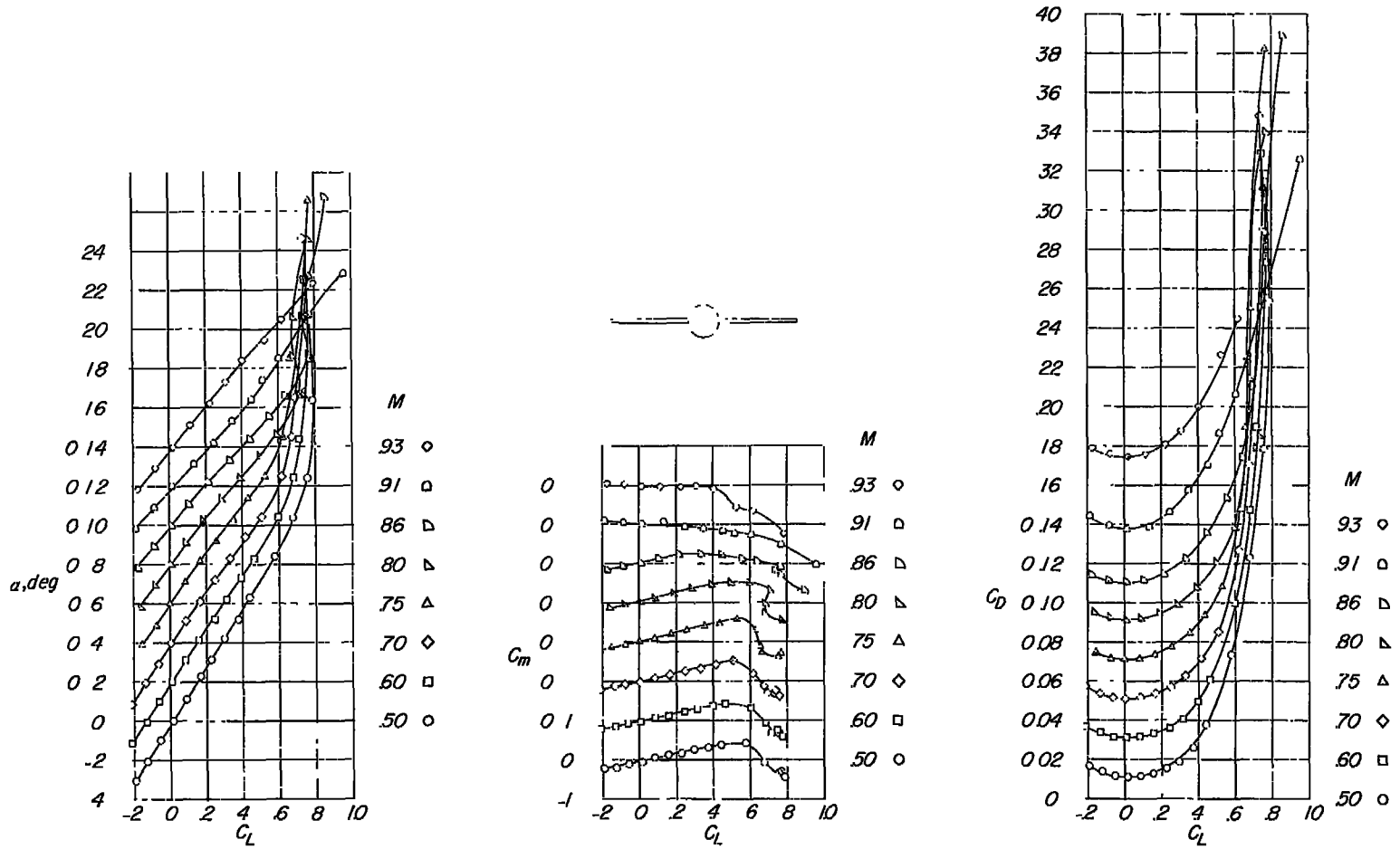
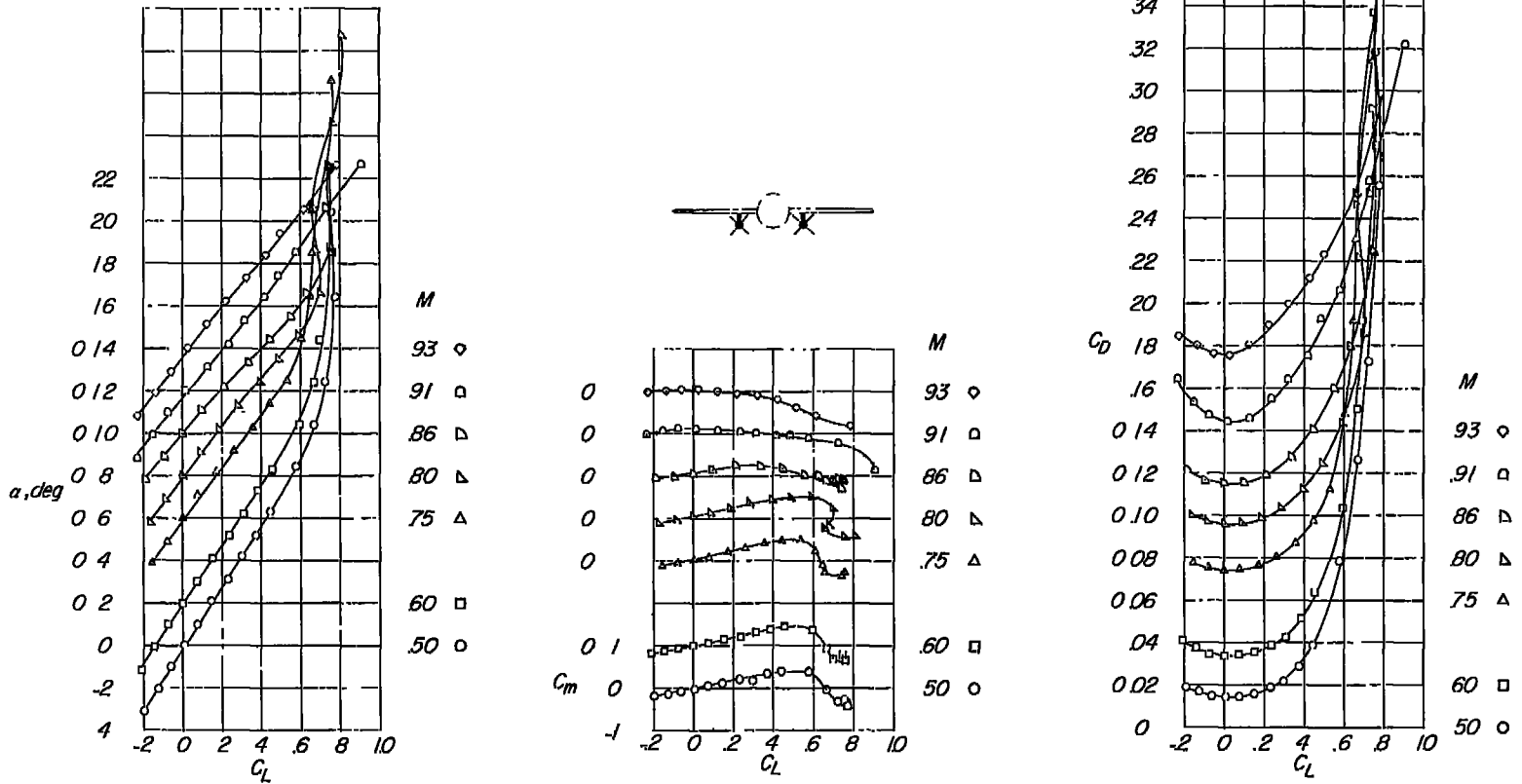
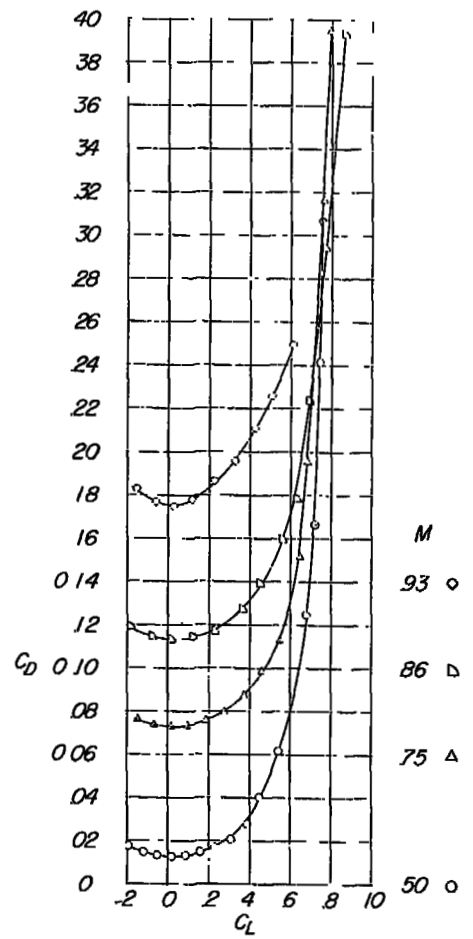
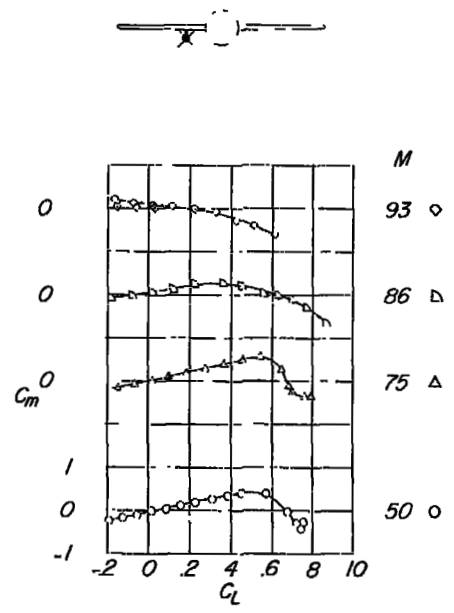
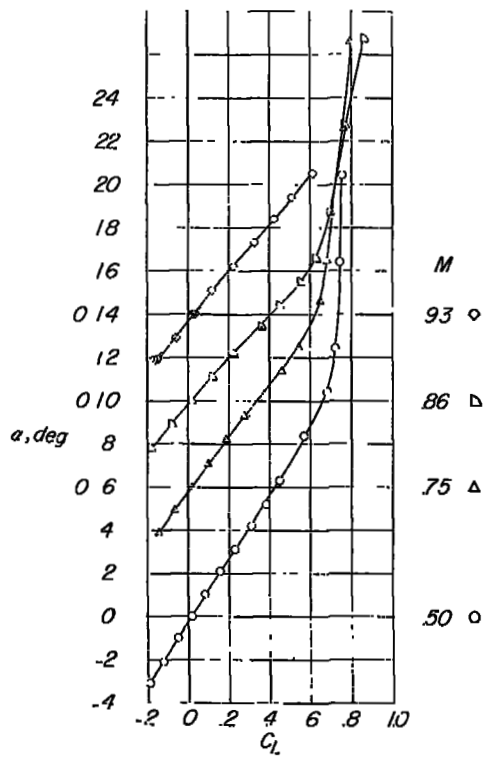


Figure 9.- Aerodynamic characteristics of the unswept-wing-fuselage combination.



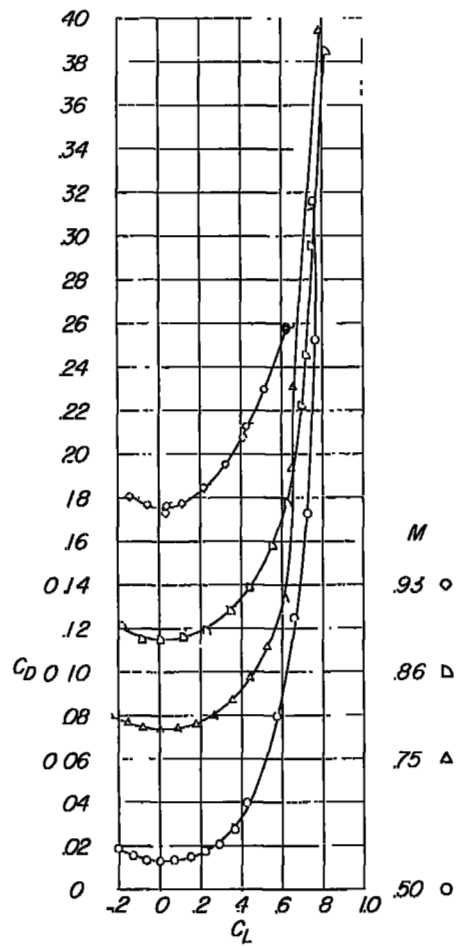
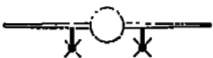
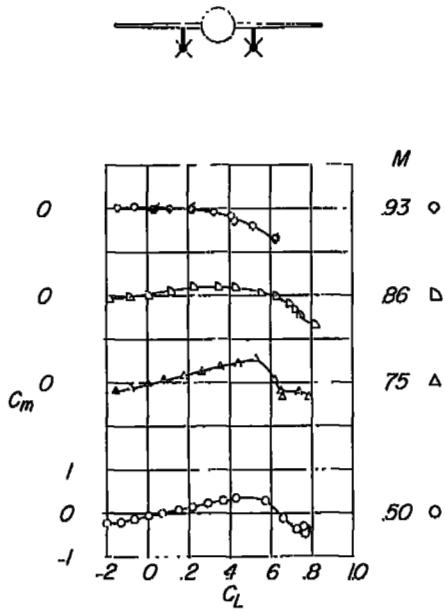
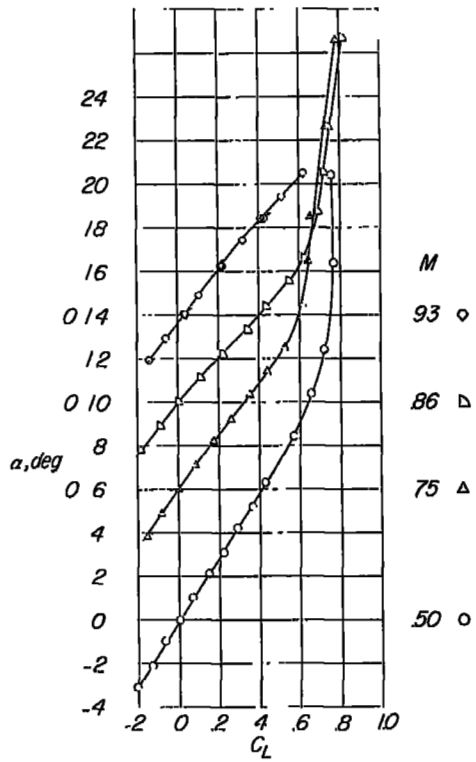
(a) Missile configuration J.

Figure 10.- Aerodynamic characteristics of the unswept-wing-fuselage model with the various configurations of the missiles.



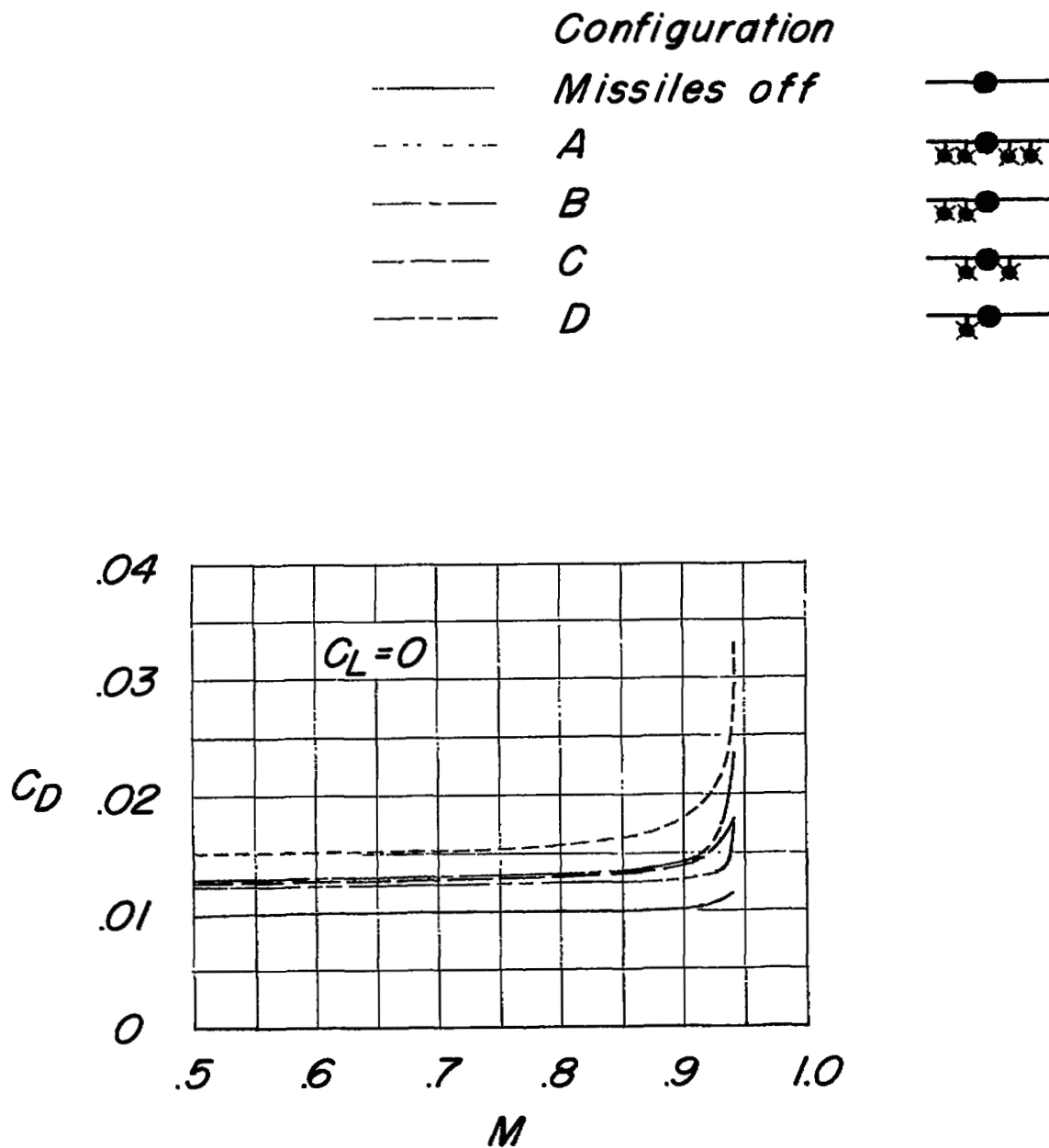
(b) Missile configuration K.

Figure 10.- Continued.



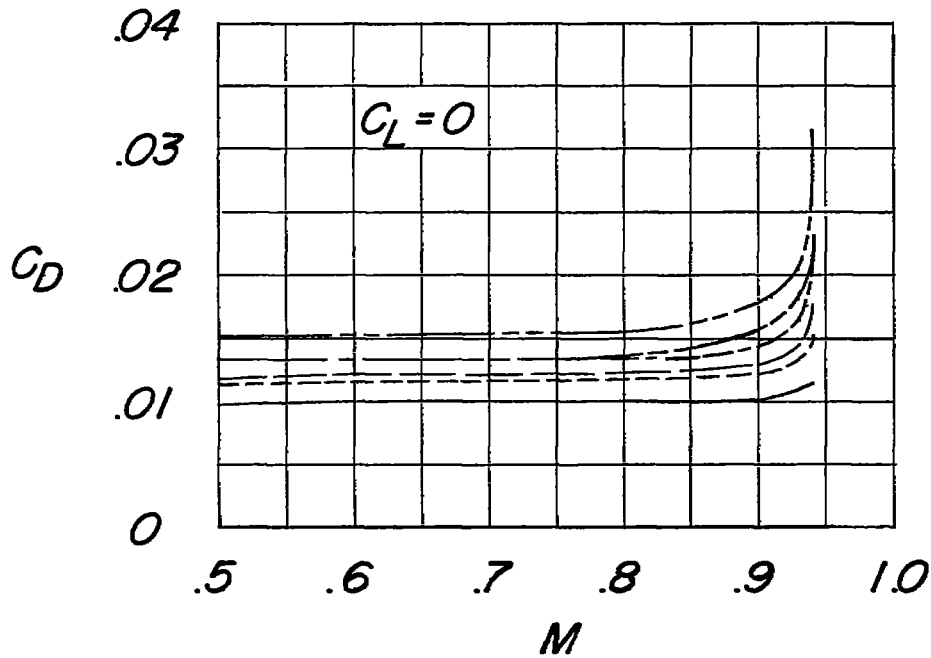
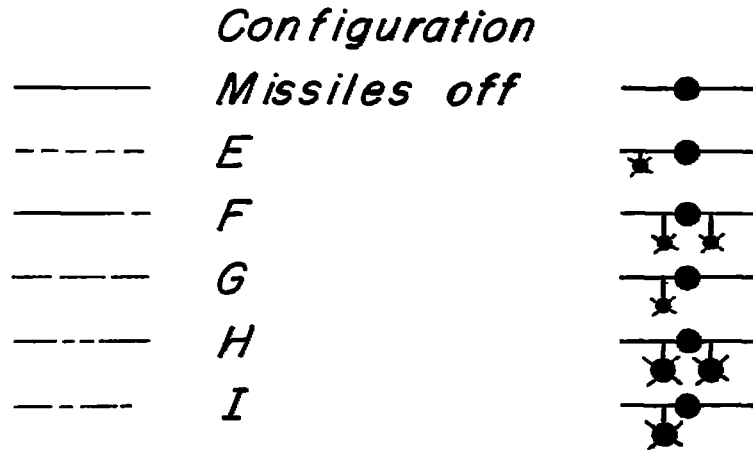
(c) Missile configuration L.

Figure 10.- Concluded.



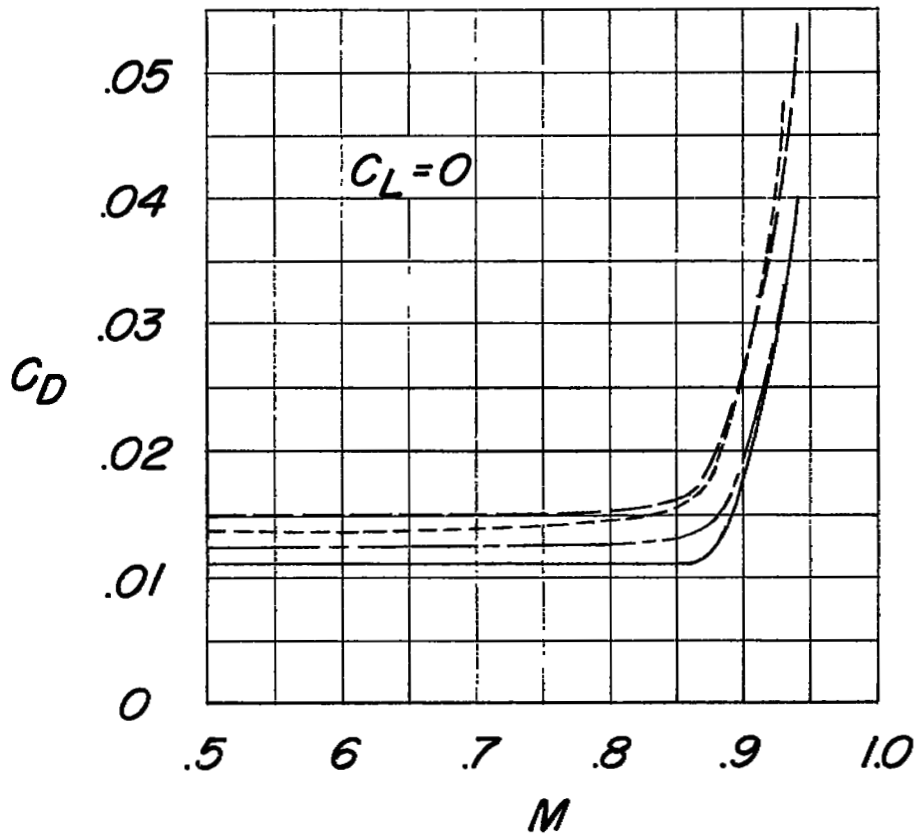
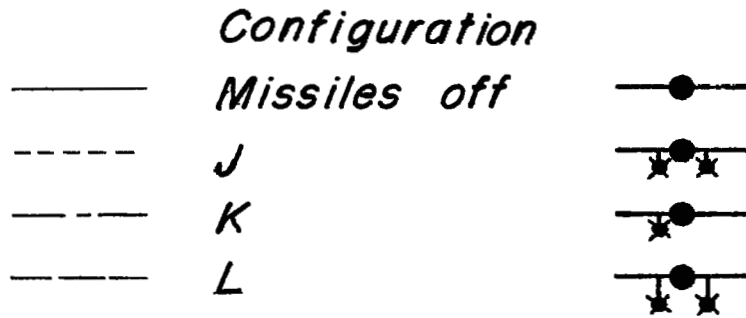
(a)  $\Lambda = 46.7^\circ$ .

Figure 11.- Drag characteristics of the model without and with the missile configurations.



(a) Concluded.

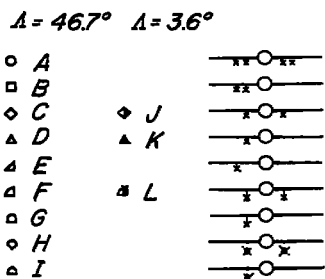
Figure 11.- Continued.



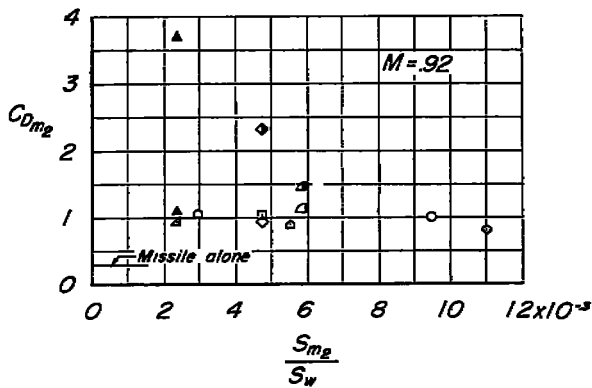
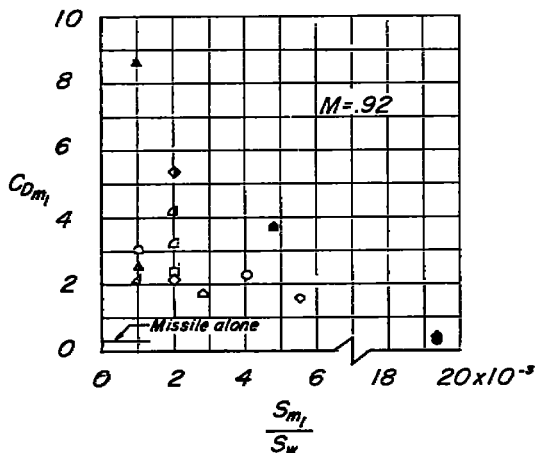
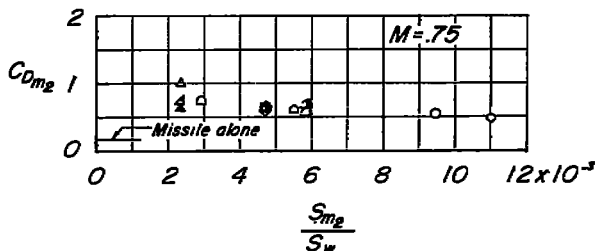
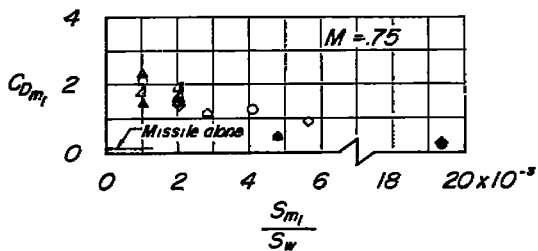
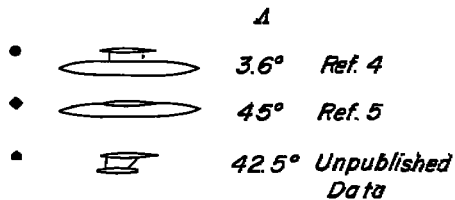
(b)  $\Lambda = 3.5^\circ$ .

Figure 11.- Concluded.

**Missile Configuration**



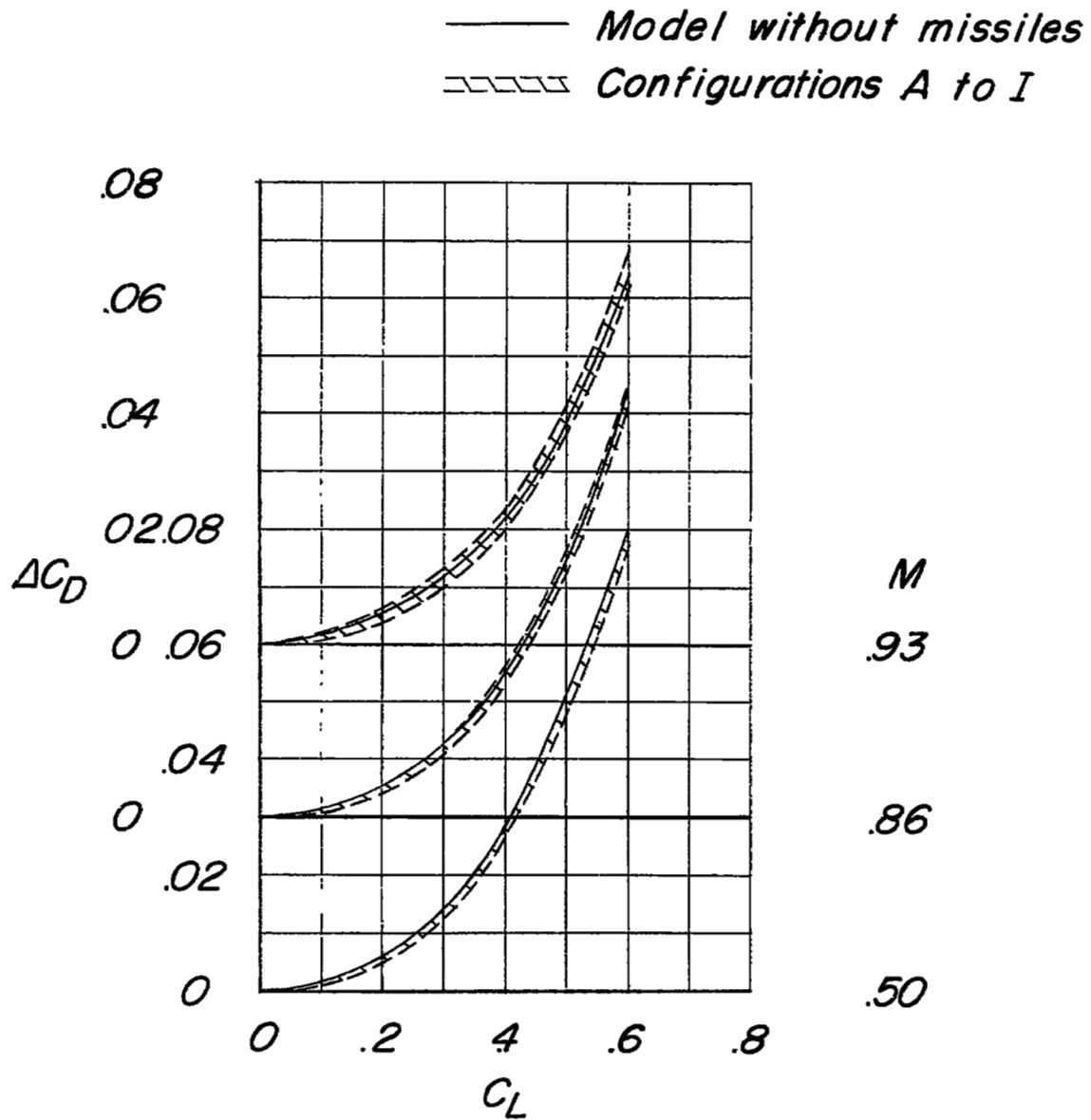
**External Stores**



(a) Based on missile-body frontal area.

(b) Based on total installation frontal area.

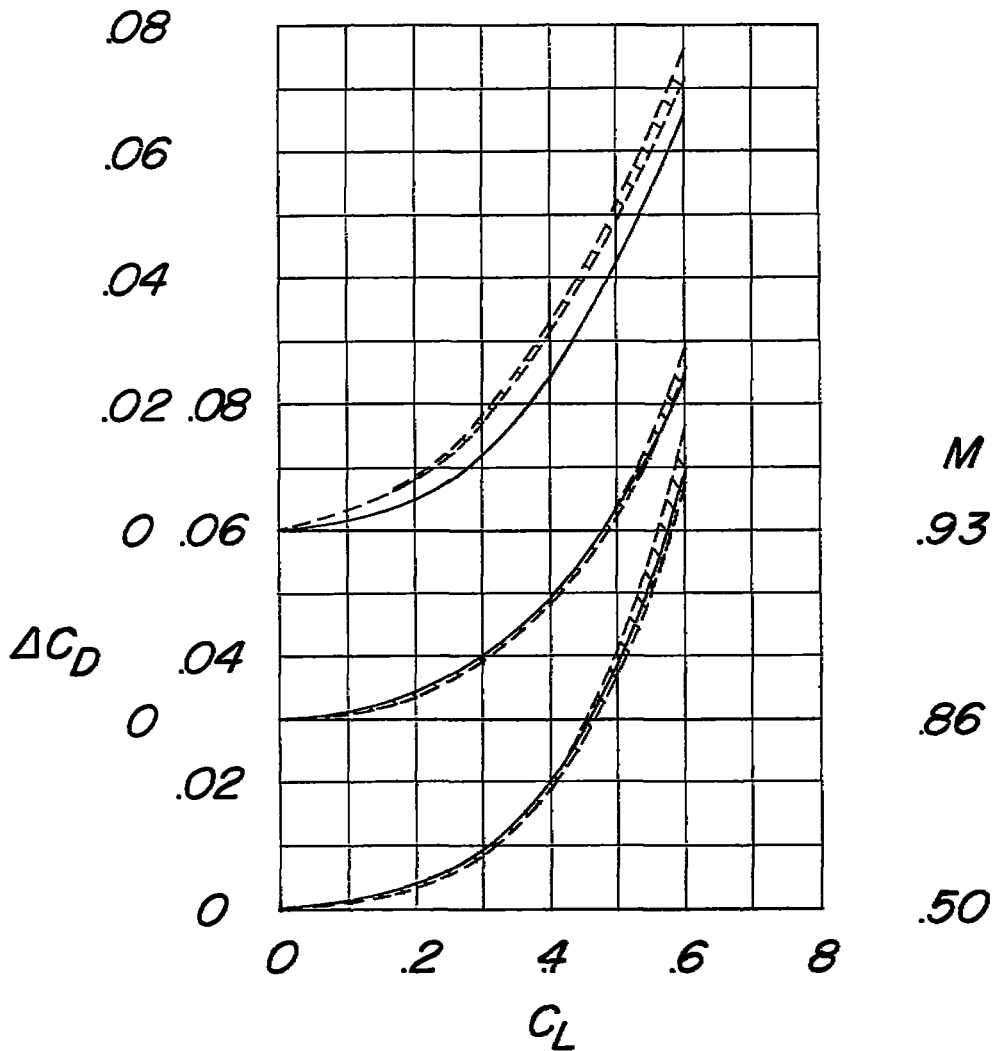
Figure 12.- Installation-drag characteristics.



(a)  $\Lambda = 46.7^\circ$ .

Figure 13.- Drag-due-to-lift characteristics of the models without and with the missile configurations.

— Model without missile  
 - - - - - Configurations J to L



(b)  $\Lambda = 3.5^\circ$ .

Figure 13.- Concluded.

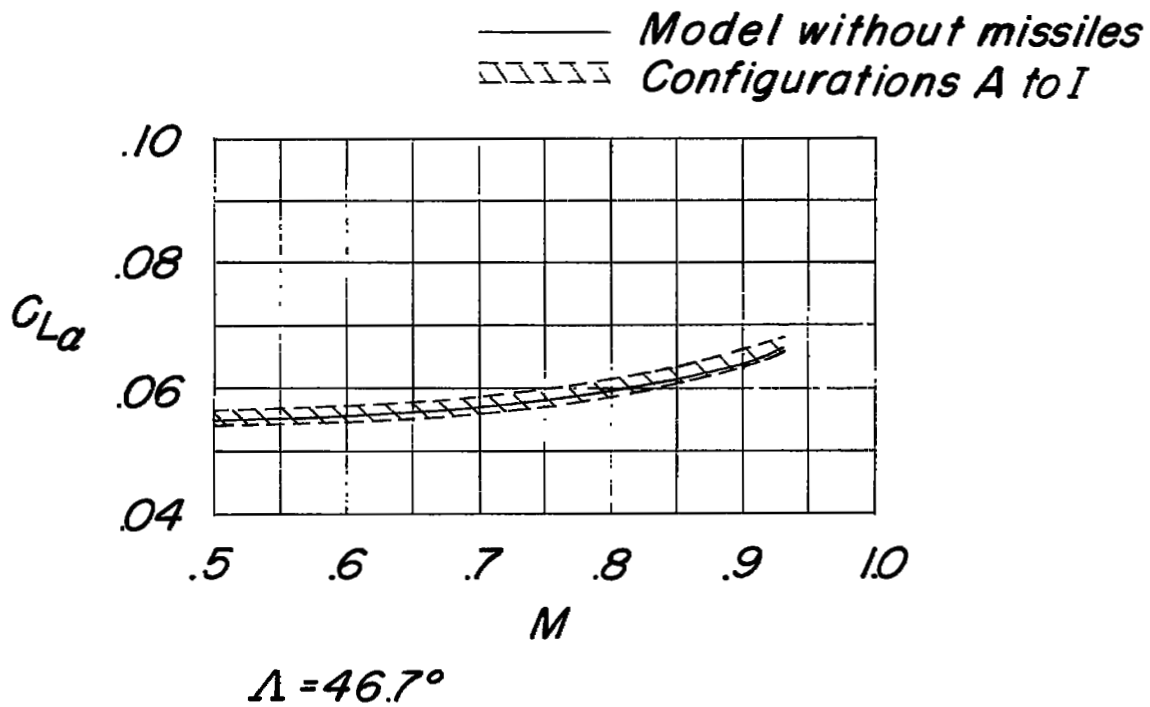
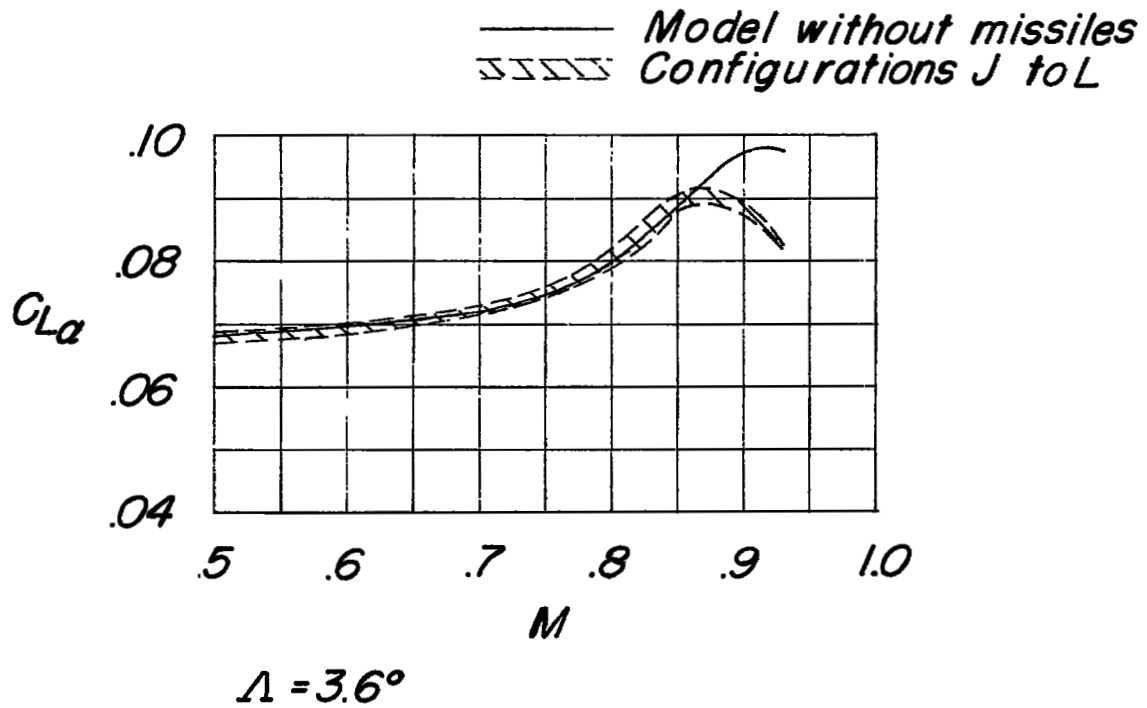
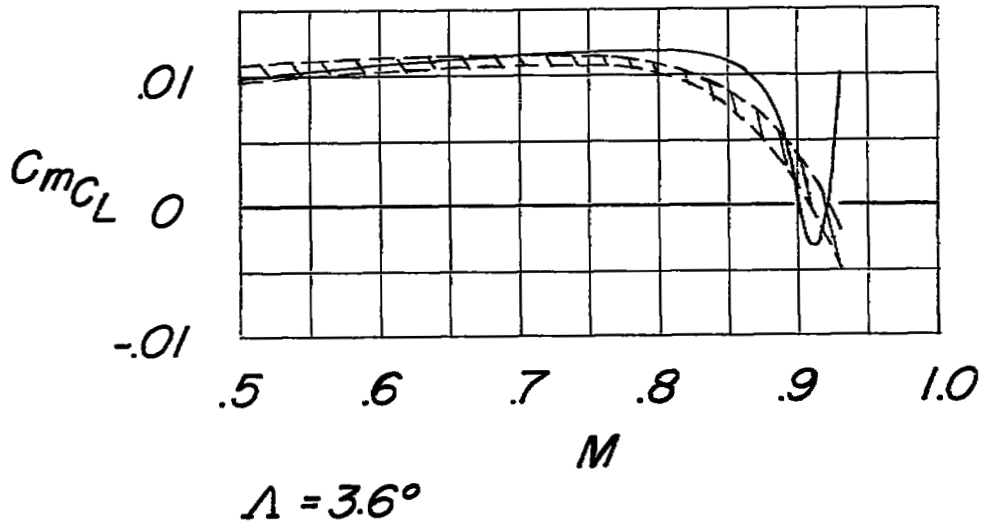


Figure 14.- Lift-curve slopes of the models without and with the missile configurations.

— Model without missiles  
 ▧▧▧▧▧ Configurations J to L



— Model without missiles  
 ▧▧▧▧▧ Configurations A to I

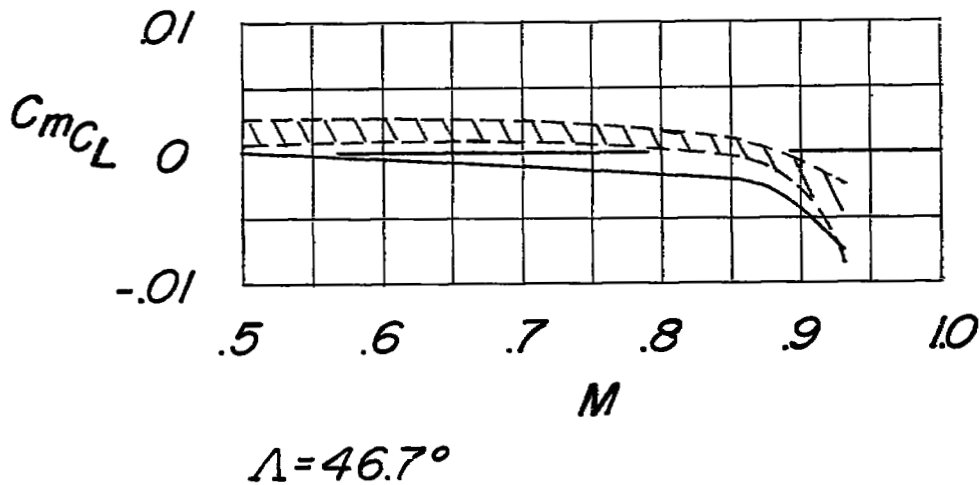


Figure 15.- Pitching-moment-curve slopes of the models without and with the missile configurations.



NASA Technical Library  
3 1176 01437 1471

